AD-A179 235 AN ANALYSIS OF SPACE STATION MOTION SUBJECT TO THE PARAMETRIC EXCITATION O (U) AIR FORCE INST OF TECH WRIGHT-PATTERSON AFB OH SCHOOL OF ENGI... J D CHAN

1/1

UNCLASSIFIED DEC 86 AFIT/GA/AA/86D-2 F/G 6/19 NL

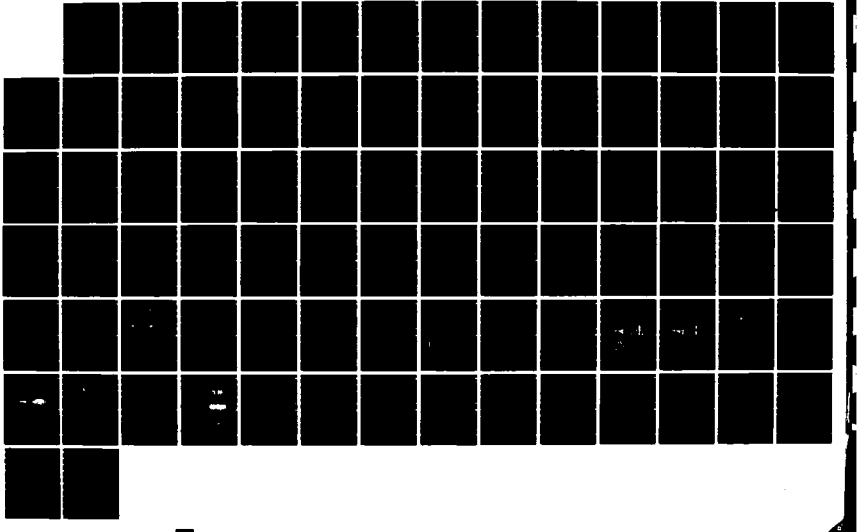

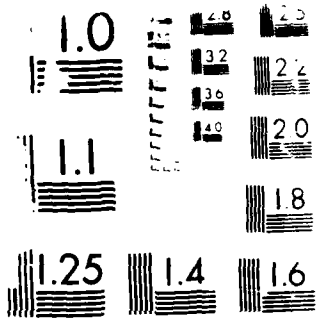
1.0
1.1
1.25
1.4
1.6
1.8
2.0
2.2
2.5
28
32
36
40

AN ANALYSIS OF SPACE STATION MOTION SUBJECT TO THE PARAMETRIC EXCITATION OF PERIODIC ELEVATOR MOTION

THESIS

John D. Chan
Second Lieutenant, USAF

AFIT/GA/AA/86D-2

DEPARTMENT OF THE AIR FORCE
AIR UNIVERSITY
AIR FORCE INSTITUTE OF TECHNOLOGY

Wright-Patterson Air Force Base, Ohio

AFIT/GA/AA/86D-2

AN ANALYSIS OF SPACE STATION MOTION SUBJECT TO THE PARAMETRIC EXCITATION OF PERIODIC ELEVATOR MOTION

THESIS

John D. Chan
Second Lieutenant, USAF

AFIT/GA/AA/86D-2

AFIT/GA/AA/86D-2

AN ANALYSIS OF SPACE STATION MOTION SUBJECT TO THE PARAMETRIC EXCITATION OF PERIODIC ELEVATOR MOTION

THESIS

Presented to the Faculty of the School of Engineering

of the Air Force Institute of Technology

Air University

In Partial Fulfillment of the

Requirements for the Degree of

Master of Science in Astronautical Engineering

John D. Chan, B.S.

Second Lieutenant, USAF

December 1986

A-1

Approved for public release; distribution unlimited

Preface

The addition of an elevator to an orbiting space station introduces time varying moments of inertia, a source of parametric excitation. This phenomenon of a parametrically excited system can also be seen when eccentricity is introduced to the orbit of a gravity gradient stabilized rigid body.

An article relevant to this study, "Stability of Rotating Space Station Containing a Moving Element," (Salimov, 1975:41-45) examined the equations of a symmetric station containing two crew members whose motion was described by either radial or circular oscillations. The study was restricted, however, to a single configuration vehicle rotating in free space. Thus, there is suitable motivation to consider a general body that contains a moving element in an inverse square gravitational field. That is the concern of the following study.

I wish to thank my thesis advisor, C.H. Spenny, of the Department of Aeronautics and Astronautics, for his continuing patience and assistance throughout the duration of this study.

John D. Chan

Computer: Atari 130XE
Software: Omniwriter
Printer: Panasonic KX-P1080

Table of Contents

List of Figures

List of Symbols

a	Semi-major Axis
a_T	Variable from Hill's Equation
A	Direction Cosine Matrix
A_{ij}	Element of Direction Cosine Matrix
B	Body Principal Basis
$\hat{b}_1, \hat{b}_2, \hat{b}_3$	Orthogonal Directions of Body Principal Basis
e	Eccentricity
$\underline{H}$	Angular Momentum of the Space Station
I	Inertia Dyadic of the Space Station When Superscripted, Refers to Inerial Frame
I_1, I_2, I_3	Principal Moments of Inertia of the Space Station about Composite Center of Mass
I_{o1}, I_{o2}, I_{o3}	Principal Moments of Inertia of the Space Station Without the Elevator about the Center of Mass
$\underline{M}$	External Gravity Torque
M_1, M_2, M_3	Body Components of $\underline{M}$
M	Reduced Elevator Mass
m_e	Mass of the Elevator
m_s	Mass of Sphere
$\underline{N}$	Vector Eccentric Orbital Rate
N	Scalar Eccentric Orbital Rate
n	Circular Orbital Rate
O	Orbit Basis
$\hat{o}_1, \hat{o}_2, \hat{o}_3$	Orthogonal Directions of Orbit Basis
p, y, r	Pitch, Yaw, and Roll Euler Angles

q_1, q_2, q_3, q_4	Variables of Hill's Equation In Appendix A, these are Euler Parameters
$\underline{q}$	Quaternion
$\underline{R}$	Vector Radius from Earth Center to Space Station Center of Mass
R_1, R_2, R_3	Body Components of $\underline{R}$
R	Scalar Magnitude of $\underline{R}$
r_0, r_1, r_2	Inertia Ratios
t	Time
t_p	Time Since Periapsis Passage
T	Dimensionless Time Variable
μ	Characteristic Exponent
u	Earth's Gravitational Constant
w	Omega, the Natural Frequency of Elevator Motion
$^I\underline{w}^B$	Angular Velocity of Space Station with Respect to an Inertial Frame
$^I\underline{w}^O$	Angular Velocity of Orbit Basis with Respect to an Inertial Frame
$^O\underline{w}^B$	Angular Velocity of Space Station with Respect to Orbit Frame
z	Transformed Pitch Variable
Z	Skew-Symmetric Matrix

Abstract

This study will derive the equations of attitude motion for a gravity gradient stabilized space station whose moments of inertia are varying with time. The equations are then linearized, after which an analytical solution of the pitch equation is developed. An examination of the stability of motion for the resulting Hill equation is presented and then compared to the solution obtained from numerical integration of the nonlinear equations. The results show that for elevator frequencies on the order of the orbit rate, motion can grow unboundedly with time. Consequently, the shape of the classical Lagrange stability region is altered.

AN ANALYSIS OF SPACE STATION MOTION SUBJECT TO THE PARAMETRIC EXCITATION OF PERIODIC ELEVATOR MOTION

I. Introduction

As the size of the space station and its platforms begin to increase, it will become necessary to provide a means for travelling from compartment to compartment. Hence, there is a need for an elevator apparatus that can shuttle mass between the separate modules. Yet, it is known that internal mass movement can affect the attitude stability of a vehicle (Salimov, 1974:30, 1975:41). Consequently, it is the objective of this study to examine the motion of a gravity gradient stabilized space station in which an elevator mechanism operates along the body axis nominally aligned to the local vertical.

To visualize the problem, refer to Fig. 1. The composite center of mass will move in a prescribed circular orbit with gravity being the only external force. It is assumed that the attitude and orbital motions are completely decoupled, and therefore each is analyzed separately. The motion of the elevator relative to the space station will be prescribed beforehand, hence, the translational motion of the elevator and the space station relative to the composite center of mass is known. Thus, with the orbit

predetermined, only the rotational motion of the space station needs to be analyzed.

II. Derivation of the Equations of Motion

The formulation of the equations of motion for a space station of arbitrary shape begins with

$$\underline{M} = {}^{I}d/dt[\underline{H}] \qquad (1)$$

where $\underline{M}$ is the external torque produced by the gravitational field, and $\underline{H}$ is the angular momentum of the space station. The superscript I indicates that the time derivative must be taken with respect to an inertial frame. The reference point about which to determine moments and angular momentum is the composite center of mass, which traces out the orbit path. Now, due to the prescribed motion of the elevator, the "geometric center" of the space station moves with respect to the composite center of mass. The angular momentum can be written

$$\underline{H} = I \cdot {}^{I}\underline{w}^{B} \qquad (2)$$

where I is the inertia dyadic of the space station. The superscript B denotes the body principal basis, $\hat{b}_1, \hat{b}_2, \hat{b}_3$, that is rigidly attached to the space station, while ${}^{I}\underline{w}^{B}$ is the inertial angular velocity of the space station with respect to an inertial frame. Since the angular momentum is calculated with the composite center of mass as reference

point, the inertia dyadic I must be evaluated in a frame of reference *not* fixed to the translating space station but attached to the center of mass. Thus, I will be a function of time, I(t). Refer to Eqs (1) and (2), and permit the vector quantities $\underline{M}$ and $\underline{w}$ to be expressed along the body principal basis, $\hat{b}_1, \hat{b}_2, \hat{b}_3$ (See Fig. 2). Insert Eq (2) into Eq (1) and obtain

$$\underline{M} = {}^{B}d/dt[I \cdot {}^{I}\underline{w}^{B}] + {}^{I}\underline{w}^{B} \times [I \cdot {}^{I}\underline{w}^{B}] \qquad (3)$$

Since I and ${}^{I}\underline{w}^{B}$ depend on time, the first term of Eq (3) becomes

$${}^{B}d/dt[I \cdot {}^{I}\underline{w}^{B}] = I\ {}^{B}d/dt[{}^{I}\underline{w}^{B}] + {}^{I}\underline{w}^{B}\ d/dt[I] \qquad (4a)$$

Or, in matrix form,

$${}^{B}d/dt[I \cdot {}^{I}\underline{w}^{B}] = \begin{bmatrix} I_1 & 0 & 0 \\ 0 & I_2 & 0 \\ 0 & 0 & I_3 \end{bmatrix} \begin{Bmatrix} \dot{w}_1 \\ \dot{w}_2 \\ \dot{w}_3 \end{Bmatrix} + \begin{bmatrix} \dot{I}_1 & 0 & 0 \\ 0 & \dot{I}_2 & 0 \\ 0 & 0 & \dot{I}_3 \end{bmatrix} \begin{Bmatrix} w_1 \\ w_2 \\ w_3 \end{Bmatrix} \qquad (4b)$$

$$= \begin{Bmatrix} I_1\dot{w}_1 + \dot{I}_1 w_1 \\ I_2\dot{w}_2 + \dot{I}_2 w_2 \\ I_3\dot{w}_3 + \dot{I}_3 w_3 \end{Bmatrix} \qquad (4c)$$

The second term of Eq (3) becomes

$$ {}^{I}\underline{w}^{B} \times [I \cdot {}^{I}\underline{w}^{B}] = \begin{vmatrix} b_1 & b_2 & b_3 \\ w_1 & w_2 & w_3 \\ I_1 w_1 & I_2 w_2 & I_3 w_3 \end{vmatrix} \tag{5a} $$

Or,

$$ {}^{I}\underline{w}^{B} \times [I \cdot {}^{I}\underline{w}^{B}] = \begin{Bmatrix} (I_3 - I_2) w_2 w_3 \\ (I_1 - I_3) w_1 w_3 \\ (I_2 - I_1) w_1 w_2 \end{Bmatrix} \tag{5b} $$

To complete Eq (3), consider gravitational torques the only input into $\underline{M}$. Using the inverse square formulation, $\underline{M}$ is given by (Wertz, 1978:567)

$$ \underline{M} = (3u/R^3)[\underline{R} \times (I \cdot \underline{R})] \tag{6} $$

where $\underline{R}$ is the vector radius from earth center to the mass center of the spacecraft, and $u = GM$ is the earth's gravitational constant. Note here that Eq (6) does not consider the gravitational coupling of the attitude motion to the orbit, because terms of order two and higher were neglected (Wertz, 1978:567). Hence, expand Eq (6) and obtain the body components of $\underline{M}$:

$$ M_1 = (3u/R^3)[(I_3 - I_2) R_2 R_3] \tag{7a} $$

$$ M_2 = (3u/R^3)[(I_1 - I_3) R_1 R_3] \tag{7b} $$

$$ M_3 = (3u/R^3)[(I_2 - I_1) R_1 R_2] \tag{7c} $$

Substituting Eqs (4), (5), and (7) into Eq (3) yields the following equations of motion, which will be denoted as Euler-type equations:

$$I_1\dot{w}_1 + \dot{I}_1 w_1 + (I_3-I_2)w_2w_3 = (3u/R^3)(I_3-I_2)R_2R_3 \quad (8)$$

$$I_2\dot{w}_2 + \dot{I}_2 w_2 + (I_1-I_3)w_3w_1 = (3u/R^3)(I_3-I_1)R_3R_1 \quad (9)$$

$$I_3\dot{w}_3 + \dot{I}_3 w_3 + (I_2-I_1)w_1w_2 = (3u/R^3)(I_2-I_1)R_1R_2 \quad (10)$$

When comparing these equations to Euler's equations for a gravity gradient stabilized, rigid body (Kaplan, 1976:201), it is apparent that the only difference is the existence of the three $\dot{I}w$ terms. These terms are present to permit the introduction of elevator motion along arbitrary axes. Moreover, note that the solution to Eqs (8), (9), and (10) will yield components of the angular velocity vector as seen from the body basis. However, the orientation of the body cannot be determined from these equations. To obtain the attitude of the spacecraft, three angles specifying the orientation are introduced, and three more differential equations for these angles are obtained.

Consider three Euler angles, pitch, yaw, and roll, or p, y, and r, respectively, in a 3-1-2 series of Euler angle rotations. This transformation references the orientation of the body basis $\hat{b}_1,\hat{b}_2,\hat{b}_3$ with respect to the orbit basis $\hat{o}_1,\hat{o}_2,\hat{o}_3$, where $\hat{o}_1$ is the direction of the local vertical,

$\hat{o}_2$ is tangent to the orbit path, and $\hat{o}_2$ is normal to the orbit plane. The associated direction cosine matrix is given by

$$A_{312}(p,y,r) = A_2(r)A_1(y)A_3(p)$$

$$= \begin{bmatrix} crcp-sysrsp & crsp+sysrcp & -cysr \\ -cysp & cycp & sy \\ srcp+sycrsp & srsp-sycrcp & cycr \end{bmatrix} \quad (11)$$

where c = cosine and s = sine.

The expressions for the rotation angles in terms of the elements of the direction cosine matrix are

$$p = -\arctan(A_{21}/A_{22}) \quad (12a)$$

$$y = \arcsin(A_{23}) \quad (12b)$$

$$r = -\arctan(A_{13}/A_{33}) \quad (12c)$$

Note that when y = 90°, p and r are associated with the same degree of freedom in the 3-1-2 sequence of rotations. In other words, the p and r rotations have a similar effect at y = 90°. (The type 3-1-2 rotation was selected because this condition of singularity is unlikely to occur except for unstable motion.)

The corresponding Euler rates for the 3-1-2 rotation are given by (Kane and others, 1983:428)

$$\begin{Bmatrix} {}^{o}w_{1}{}^{s} \\ {}^{o}w_{2}{}^{s} \\ {}^{o}w_{3}{}^{s} \end{Bmatrix} = \begin{Bmatrix} \dot{p}\cos(y)\sin(r) + \dot{y}\cos(r) \\ \dot{p}\sin(y) + \dot{r} \\ \dot{p}\cos(y)\cos(r) + \dot{y}\sin(r) \end{Bmatrix} \tag{13}$$

which are the body components of ${}^{o}\underline{w}^{s}$, the angular velocity of the space station with respect to the orbit basis. The angular velocity with respect to the inertial basis, ${}^{I}\underline{w}^{s}$ is needed. Therefore,

$${}^{I}\underline{w}^{s} = {}^{I}\underline{w}^{o} + {}^{o}\underline{w}^{s} \tag{14}$$

And since the angular velocity of the orbit basis with respect to the inertial frame, ${}^{I}\underline{w}^{o}$, is equal to $N\hat{o}_{3}$, the eccentric orbital rate, Eq (14) takes the form

$$\begin{Bmatrix} w_{1} \\ w_{2} \\ w_{3} \end{Bmatrix} = \begin{bmatrix} A_{11} & A_{12} & A_{13} \\ A_{21} & A_{22} & A_{23} \\ A_{31} & A_{32} & A_{33} \end{bmatrix} \begin{Bmatrix} 0 \\ 0 \\ N \end{Bmatrix} + \begin{Bmatrix} \dot{p}\cos(y)\sin(r) + \dot{y}\cos(r) \\ \dot{p}\sin(y) + \dot{r} \\ \dot{p}\cos(y)\cos(r) + \dot{y}\sin(r) \end{Bmatrix} \tag{15}$$

Or,

$$w_{1} = A_{13}N + \dot{p}\cos(y)\sin(r) + \dot{y}\cos(r) \tag{16a}$$

$$w_{2} = A_{23}N + \dot{p}\sin(y) + \dot{r} \tag{16b}$$

$$w_{3} = A_{33}N + \dot{p}\cos(y)\cos(r) + \dot{y}\sin(r) \tag{16c}$$

The Euler angle rates can now be solved for in terms of

angular velocity and Euler angles:

$$\dot{p} = [(w_3 - A_{33}N)\cos(r) - (w_1 - A_{13}N)\sin(r)]\sec(y) \quad (17a)$$

$$\dot{y} = (w_1 - A_{33}N)\cos(r) + (w_3 - A_{33}N)\sin(r) \quad (17b)$$

$$\dot{r} = -[(w_3 - A_{33}n)\cos(r) - (w_1 - A_{12}N)\sin(r)]\tan(y) + (w_2 - A_{23}N) \quad (17c)$$

Since the torque components appearing in the Euler-type equations, Eqs (8), (9), and (10), are functions of the inertial orientation of the body, they must be solved simultaneously with Eqs (17a), (17b), and (17c). This results in a problem consisting of six first order, nonlinear differential equations.

Parameterization of the attitude could also be carried out in terms of Euler symmetric parameters q_1, q_2, q_3, and q_4 instead of Euler angles. With Euler parameters, there are four kinematic equations of motion that must be solved in conjunction with Eqs (8), (9), and (10). Their derivation as well as the parameterization of the direction cosine matrix in terms of the quaternion $\underline{q}$ is demonstrated in Appendix A.

III. Linearization

In Eqs (8), (9), and (10), the Euler-type equations for a space station with elevators operating along arbitrary axes, there exist the terms $\dot{I}_1$, $\dot{I}_2$, and $\dot{I}_3$. If elevator motion soley occurs along the yaw axis, then the term $\dot{I}_1$ vanishes. The significance of this configuration lies in the fact that Liapunov stability analysis requires the following equilibrium position of the space station: The axis of minimum moment of inertia, or minor axis, must be aligned to the local vertical, while the major axis of maximum inertia must be perpendicular to the orbit (Hughes, 1986:296,298). So, if the elevator is to travel along the longest axis of the space station inertia ellipsoid, then it will operate along the body $\hat{b}_1$ direction. Hence, with $\dot{I}_1 = 0$, Eqs (8), (9), and (10) become

$$I_1\dot{w}_1 + (I_3-I_2)w_2w_3 = (3u/R^3)(I_3-I_2)R_2R_3 \qquad (18a)$$

$$I_2\dot{w}_2 + \dot{I}_2w_2 + (I_1-I_3)w_3w_1 = (3u/R^3)(I_1-I_3)R_3R_1 \qquad (18b)$$

$$I_3\dot{w}_3 + \dot{I}_3w_3 + (I_2-I_1)w_1w_2 = (3u/R^3)(I_2-I_1)R_1R_2 \qquad (18c)$$

Now consider small amplitude motions about the equilibrium position. The direction cosine matrix, Eq (11), becomes, for small angles,

$$A(p,y,r) = \begin{bmatrix} 1 & p & -r \\ -p & 1 & y \\ r & -y & 1 \end{bmatrix} \tag{19}$$

Consequently, the radius vector, $\underline{R}$, can be written in body components as

$$\begin{Bmatrix} R_1 \\ R_2 \\ R_3 \end{Bmatrix} = \begin{bmatrix} 1 & p & -r \\ -p & 1 & y \\ r & -y & 1 \end{bmatrix} \begin{Bmatrix} R \\ 0 \\ 0 \end{Bmatrix} \tag{20}$$

Or,

$$\begin{Bmatrix} R_1 \end{Bmatrix} = \begin{Bmatrix} R \end{Bmatrix} \tag{21a}$$

$$\begin{Bmatrix} R_2 \end{Bmatrix} = \begin{Bmatrix} -Rp \end{Bmatrix} \tag{21b}$$

$$\begin{Bmatrix} R_3 \end{Bmatrix} = \begin{Bmatrix} Rr \end{Bmatrix} \tag{21c}$$

Also, observe that the orbit bases $\hat{o}_1$, $\hat{o}_2$, $\hat{o}_3$, rotates at an inertial angular velocity $\underline{N} = N\hat{o}_3$. This can be expressed in body coordinates

$${}^{\prime}\underline{w}^{o} = \begin{bmatrix} 1 & p & -r \\ -p & 1 & y \\ r & -y & 1 \end{bmatrix} \begin{Bmatrix} 0 \\ 0 \\ N \end{Bmatrix} \tag{22a}$$

$$= \begin{Bmatrix} -rN \\ yN \\ N \end{Bmatrix} \tag{22b}$$

Note that the body rates relative to the orbit basis can be expressed as

$$ {}^{o}\underline{w}^{B} = \dot{q}\hat{b}_1 + \dot{r}\hat{b}_2 + \dot{p}\hat{b}_3. \tag{23} $$

When components are equated in Eq (14), ${}^{I}\underline{w}^{B}$ becomes

$$ w_1 = -rN + \dot{y} \tag{24a} $$

$$ w_2 = yN + \dot{r} \tag{24b} $$

$$ w_3 = N + \dot{p} \tag{24c} $$

Take a time derivative derivative in the body frame of Eqs (24a), (24b) and (24c), and the result takes the form

$$ \dot{w}_1 = \ddot{y} - (\dot{r}N + r\dot{N}) \tag{25a} $$

$$ \dot{w}_2 = \ddot{r} + (\dot{y}N + y\dot{N}) \tag{25b} $$

$$ \dot{w}_3 = \ddot{p} + \dot{N} \tag{25c} $$

Let N and R, for small eccentricity e, be approximated (Kaplan, 1976:202)

$$ N = n[1 + 2e\cos(nt_p)] \tag{26} $$

$$ R = a[1 - e\cos(nt_p)] \tag{27} $$

where $n = (u/a)^{1/2}$ is the mean motion, and t_p is the ti

since periapsis passage. (Recall that the mean anomaly M = nt_p.) Next, differentiate Eq (26) with respect to time and obtain

$$\dot{N} = -2n^2 e \sin(nt_p) \tag{28}$$

Finally, substitute Eqs (21), (24), and (25) into Eqs (18a), (18b), and (18c), and write the result as

$$I_1(\ddot{y}-\dot{r}N-\dot{N}r)+(I_3-I_2)(\dot{r}+yN)(\dot{p}+N) = (3u/R^5)(I_3-I_2)(-pR)(rR) \tag{29}$$

$$I_2(\ddot{r}+\dot{y}N+\dot{N}y)+\dot{I}_2(\dot{r}+yN)+(I_1-I_3)(\dot{p}+N)(\dot{y}-rN) = (3u/R^5)(I_1-I_3)(rR)(R) \tag{30}$$

$$I_3(\ddot{p}+\dot{N})+\dot{I}_3(\dot{p}+N)+(I_2-I_1)(\dot{y}-rN)(\dot{r}+yN) = (3u/R^5)(I_2-I_1)(R)(-pR) \tag{31}$$

Substitute for N and $\dot{N}$ from Eqs (26) and (28), and delete the products of quantities assumed to be small, such as $\dot{p}y$ and pe. Then, substitute $u/R^3 = N^2$ into the above, and Eqs (29), (30), and (31) can be rewritten

$$I_1\ddot{y} + (I_3-I_2-I_1)n\dot{r} + (I_3-I_2)n^2y = 0 \tag{32}$$

$$I_2\ddot{r} + (I_2+I_1-I_3)n\dot{y} - 4(I_1-I_3)n^2r + \dot{I}_2(\dot{r}+yn) = 0 \tag{33}$$

$$I_3[\ddot{p}-2n^2e\sin(nt_p) + 3n^2(I_2-I_1)p + \dot{I}_3(\dot{p}+n) = 0 \tag{34}$$

These equations are nearly identical to those derived by Kaplan for a gravity gradient stabilized rigid body (Kaplan,

1976:204). The only difference is the existence of the $\dot{I}$ terms due to elevator movement along the yaw axis. Also, note that the pitch equation, Eq (34), is uncoupled from the coupled yaw and roll equations, Eqs (32) and (33).

If the analysis were carried out with elevator motion along all three axes, the character of the equations would remain the same. This is because the $\dot{I}_t w_t$ term that was eliminated in Eq (18a) would appear as $\dot{I}_t(-r\eta+\dot{y})$ in Eq (32), which would add to the yaw-roll coupling already present in Eqs (32) and (33).

IV. Analysis of the Linearized Pitch Equation

Variable Transformation

Since the pitch equation is decoupled from the roll and yaw equations, deriving an analytical solution for pitch motion becomes the immediate aim. Hence, insert the expression for N from Eq (26) into Eq (34), divide by I_3, rearrange, and obtain

$$\ddot{p} + (\dot{I}_3/I_3)\dot{p} + 3n^2[(I_2-I_1)/I_3]p + (\dot{I}_3/I_3)n = 2n^2 e\sin(nt_p) \quad (35)$$

Now, define the following:

$$P(t) = (1/2)(\dot{I}_3/I_3) \quad (36)$$

$$R^2(t) = 3n[(I_2-I_1)/I_3] \quad (37)$$

$$Q(t) = -(\dot{I}_3/I_3)n + 2n^2 e\sin(nt_p) \quad (38)$$

Substituting these expressions into Eq (35) yields this linear, second order equation:

$$\ddot{p} + 2P(t)\dot{p} + R^2(t)p = Q(t) \quad (39)$$

Introduce a variable transformation, defined by

$$z = p \exp[\int P dt] \quad (40)$$

Consequently, p can be written as

$$p = z \exp[-\int P dt] \tag{41}$$

The necessary time derivatives, $\dot{p}$ and $\ddot{p}$ are

$$\dot{p} = e^{-\int P dt}[\dot{z} - Pz] \tag{42}$$

$$\ddot{p} = e^{-\int P dt}[-2\dot{z}P + zP^2 - z\dot{P} + \ddot{z}] \tag{43}$$

Inserting p, $\dot{p}$, and $\ddot{p}$ into Eq (35) yields

$$\ddot{z} + [R^2 - P^2 - \dot{P}]z = Qe^{\int P dt} \tag{44}$$

where P, Q, and R are given in Eqs (36), (37), and (38). The above is a linear equation in which the coefficient of z is a function of time. In fact, if elevator motion is chosen to be sinusoidal, then the coefficient of z is a periodic function of time. Appendix B, accordingly, details the expansion of this coefficient as well as demonstrate the final form of the transformed, homogeneous pitch equation to be

$$z'' + [a_7 + 16q_1\cos 2T + 16q_2\cos 4T + 16q_3\cos 6T + 16q_4\cos 8T]z = 0 \tag{45}$$

where

$$a_T = 3(n/w)^2[r_2-r_1+(r_o/2)] + (3/2)(n/w)^2r_o(r_1-r_2) + (9/8)(n/w)^2r_o^2(r_2-r_1-1) + (13/8)r_o^2 - (13/8)r_o^3 + (273/128)r_o^4 + (15/16)(n/w)^2r_o^3 \quad (46)$$

$$q_1 = (1/16)[(-3/2)(n/w)^2r_o^2(r_2-r_1) + (3/2)(n/w)^2r_o(r_2-r_1) - (45/32)(n/w)^2r_o^3 + (3/2)(n/w)^2r_o^2 - (3/2)(n/w)^2r_o - (93/32)r_o^4 + (3/2)r_o^3 + r_o^2/2 - r_o] \quad (47)$$

$$q_2 = (1/16)[(3/8)(n/w)^2r_o^2(r_2-r_1-1) + (27/32)r_o^4 + (9/16)(n/w)^2r_o^3 - (1/8)(r_o^2 + (1/8)r_o^3] \quad (48)$$

$$q_3 = (1/16)[(-3/32)(n/w)^2r_o^3 + (3/32)r_o^4] \quad (49)$$

$$q_4 = (3/2048)r_o^4 \quad (50)$$

and where n is the orbit rate, and w is the frequency of elevator motion. The variables $r_1 = I_{o1}/I_{o3}$ and $r_2 = I_{o2}/I_{o3}$ are ratios of principal moments of inertia about the center of mass of the space station without an elevator. The ratio $r_o = ML^2/4I_{o3}$ is the effective elevator inertia divided by the space station pitch inertia.

The above equation in z is a form of Hill's equation,

$$\ddot{z} + [a_T + \sum_i q_i(t)]z = 0 \quad (51)$$

where $q_i(t)$ is a periodic function (Meirovitch, 1970:280).

This type of forced motion, in which $g_i(t)$ acts as an energy source, is an instance of parametric excitation. It is important, in the analysis of the stability of this motion, to determine what values of a_T and $g_i(t)$ in Eq (51) yield unbounded solutions of the system.

Mathieu's Equation

Since the theory of Hill's equations has been thoroughly investigated, the results can be immediately applied to the parameters of the present problem. A special case of Hill's equation, Mathieu's equation (Hayashi, 1964:87),

$$z'' + (a_T+16q\cos 2T)z = 0 \qquad (52)$$

yields a Strutt diagram similar to the one shown in Fig. 3, in which there is a partitioning of regions of stability and instability that are symmetric with respect to the horizontal axis. For the present problem, a solution is defined to be unstable if it grows unboundedly as time tends to infinity. And on the other hand, a solution is defined to be stable if it remains bounded as time tends to infinity. Further, the variables a_T and q are functions of r_0, r_1, r_2, and (n/w), as can be seen from Eqs (46) through (50). In other words, the placement of points within the stable or unstable zones of the Strutt diagram depend on the vehicle inertia shape (r_1, r_2), orbit rate to elevator

frequency (n/w), and the ratio of effective elevator inertia to pitch inertia r_o.

To carry out the stability analysis for the transformed pitch equation, one might use the fact that both the Hill and Mathieu equations are linear. Therefore, instability effects in the Hill equation can be examined via Mathieu theory by inserting the multiple q_i "Hill" terms into the Mathieu equation one at a time. This, of course, will yield only a rough approximation to the actual Strutt diagram associated with Hill's equation. The exact stability charts will be obtained when the complete nonlinear equations are numerically integrated, which will be demonstrated in Section V.

Mapping of Points on the Strutt Diagram

Since the orbiting station considered here utilizes only passive, gravity gradient stabilization for control, it is apparent that the only inertia shapes to be considered for the problem at hand are those which lie in the classical Lagrange and Delp regions, as shown in Fig. 4. For a rigid body in a circular orbit, the Lagrange region is Liapunov stable, even for finite motions, whereas the Delp region is gyrically stable (Hughes, 1986:297). Any inertia shape, i.e., any combination of (r_1,r_2) ratios that lies outside of these regions would result in unstable motion, even with the elevator stopped. Moreover, when flexibility effects are considered with a quasi-rigid body, the Delp region loses

its gyrically stable character while the Lagrange region becomes asymptotically three-axis stable (Hughes, 1986:318). At the same time, having an elevator moving along the $\hat{b}_1$ axis of a space station whose inertia shape is located in the Delp region would correspond to elevator motion along the shortest axis of the space station inertia ellipsoid. Accordingly, the Delp region will not be considered in this analysis.

To map the Lagrange region into the a_r-q_j (j=1,2,3,4) plane, Eqs (46) through (50) are used. To carry this out, the following parameters are chosen:

1. r_o: $0 \leq r_o \leq 0.25$
2. w: $n \leq w \leq \infty$

The lower limit $r_o = 0$ denotes a null elevator mass. The upper limit $r_o = 0.25$ corresponds to the elevator mass being equal to a single sphere mass of a dumbell configuration space station. The elevator frequency being equal to the orbit rate, $w = n$, sets a reasonable lower bound on elevator speed.

For each a_r-q_j diagram, the entire range of r_o values are plotted, and therefore all reasonable elevator masses are taken into account. For each value of elevator frequency, w, there is a different Strutt diagram. Typical results are shown in Fig. 5 and Fig. 6 for $w = n$.

As can be seen in Fig. 5, the Strutt diagram in the

a_1-q_1 plane for w = n, a polygon shape takes form beneath the horizontal axis when the entire range of r_o is considered. In particular, for a single r_o value, the Lagrange region that is triangular in r_1-r_2 space maps into a line in the a_1-q_1 plane (See Fig. 8). Conversely, a point in the two dimensional a_1-q_1 plane will transform into a line segment in the r_1-r_2 mapping, since several inertia shapes give rise to the same a_1-q_1 point.

Refer now to Fig. 6, the Strutt diagram in the a_1-q_2 plane for w = n. Observe that the totality of feasible space station-elevator points -- of which none are located in the unstable region -- lie very close to the horizontal axis. In fact, increasing the elevator frequency, w, to a large value will condense the locus of space station-elevator shapes from the slender region shown to a spot at the origin. (This will be demonstrated later.)

Hence, look now at the last two q variables, q_3 and q_4, and notice that they are functions of r_o, and not r_1 and r_2. The largest absolute value of either q_3 or q_4 is 6.87×10^{-4} when $r_o = 0.25$ and w = n. Thus, it is seen that q_3 and q_4 are very small.

On the whole, take into account the facts presented in the preceding paragraph as well as the actuality of no points falling in the second, third, or higher unstable regions according to the bounds set on elevator frequency, and the conclusion is made that only the first unstable zone in the a_1-q_1 plane need be considered.

Effect of Varying Elevator Frequency

Turn to Fig. 7, which demonstrates the effect of changing elevator frequency on the locus of space station-elevator points. As w is decreased from a value equal to ten times the orbit rate, 10n, to n, the first occurrence of instability appears at w = 1.9n. Thus, w = 1.9n sets an approximate ceiling on elevator frequency at which unstable motion can still occur. Or, from the other viewpoint, w = 1.9n establishes an approximate lower bound in which stable motion takes place.

Stability Predictions

A determination of the stability of the decoupled pitch motion can be predicted from the analytical solution. In Fig. 8, at $r_o = 0.25$, points 1 and 7 represent the "fence posts" enclosing points of instability. In fact, the image of points 1 and 7 in the r_1-r_2 plane are the lines 1 and 7, which also are boundaries defining the approximate zone of instability, as illustrated in Fig. 9. This is because points 1 and 7 enclose the widest range of a_r values, which are proportional to the square of pitch natural frequency. Hence any point lying outside of the zone defined by lines 1 and 7, for $r_o = 0.25$ and w = n, should result in bounded pitch motion.

For a smaller value of r_o, the predicted unstable region of Fig. 9 shrinks in width as the lines that are labeled line #1 and line #7 for $r_o = 0.25$ approach each

other as r_o is decreased. The unstable region will disappear completely when $r_o = 0$, when no elevator exists.

In Fig. 10 and Fig. 11, the prediction charts for an elevator frequency of $w = 1.3n$ is shown. When comparing Fig. 9 with Fig. 11, it is apparent that as the elevator frequency is increased, the location of the predicted unstable region shifts. In fact, as the elevator frequency approaches $w = 1.9n$, the predicted unstable region migrates toward the lowest corner of the Lagrange region, for which the only shapes that result in unstable motion are "pole" shaped space stations. For elevator frequencies greater than $w = 1.9n$, linear theory, using Mathieu's equation to approximate Hill's equation for the first unstable region, predicts no parametrically induced instability.

Refer to Fig. 12 and Fig. 13 to see the effects of an elevator frequency $w = (1/2)n$ that's less that the previously set lower bound of $w = n$. As can be seen in Fig. 12, there exist unstable points in three unstable regions, which result in three pieces being cut out of the Lagrange region in Fig. 13. (It is important to note here that the Strutt diagram shown in Fig. 12 takes into account only the q_1 term of the Hill equation when plotting the transition curves.) The shaded area in Fig. 12 represents the locus of shapes for q_2, which has been included in this a_1-q_1 plot in order to demonstrate the fact that whatever shapes yield q_2 instability will likewise yield q_1 instability.

The next section, Analysis of the Nonlinear Pitch

Equation, will test the validity of some of the previous statements made on instability by numerically integrating the nonlinear equations of motion, Eqs (17a), (17b), (17c), (18a), (18b), and (18c).

V. Analysis of the Nonlinear Pitch Equation

In the following cases, an altitude of 150 km in a low earth orbit was chosen, which yields a circular orbit rate n = 1.197×10^{-3} sec^{-1} and a period of 5,250 seconds. Several of the results -- points 2, 4, and 12 of Fig. 15, points 13, 15, and 20 of Fig. 16, points 28, 32, and 41 of Fig. 19, and the three left-hand graphs of Fig. 22 -- are graphically displayed only for a period of 100 orbits in order to demonstrate the unique oscillatory shapes, even though all points were run for a period of 1000 orbits. The remaining graphs of those same Figs. 15, 16, 19, and 22 display results for a period of 1000 orbits in order to demonstrate the unstable character of motion.

The length of elevator travel along the yaw axis was chosen to be 90 meters. Thus, an elevator frequency equal to the orbit rate, w = n, corresponds to the elevator mechanism travelling at 0.1143 ft/sec. Also, due to space limitation, only one full size figure, Fig. 14, which sets the standard for all the pitch vs. time graphs, was included.

Case #1: (w = n)

For the case of elevator frequency equal to the orbit rate, 3 "levels" of r_o were analyzed (See Fig. 8). The results are shown in Figures 15 through 18. Note that no

sequence of figures for $r_o = 0.1$ is included because no unstable cases within an integration time of 1000 orbits could be located. However, the sequence of plots for $r_o = 0.1$ seen by this author would indicate that an instability occurs at point #24. Also, since the points located at the level $r_o = 0.1$ are the closest to the horizontal axis, the theory of Mathieu equations indicates that unbounded motion caused by $e^{\mu t}$, where μ is the characteristic exponent, would occur after a longer duration of time since the magnitude of μ grows as the horizontal axis is approached.

In brief, it can be easily seen in Fig. 16 that the linearized, analytical solution gives a fair approximation to the numerical result, which is shown shaded. The difference in shape between the predicted region of instability and the resulting region gotten from numerical integration is attributable to the nonlinearity of the equations of motion, seen in Eqs (8), (9), and (10). Further, when comparing Fig. 18 to Fig. 11, it is seen that the resulting zone of instability is "shifted lower" than the predicted solution.

Case #2: ($w = 1.3n$)

For elevator frequency equal to 1.3 times the orbit rate, the results, carried out for a single $r_o = 0.25$, are shown in Figures 19, 20, and 21. The predicted unstable region (Fig. 20) is less accurate than for case #1.

Case #3: Effect of Elevator Motion in 3 Dimensions

One significant test case involving roll and yaw motion is shown in Fig. 20. The three left-hand graphs display the effect of simple internal resonance in the Lagrange region, which causes bounded exchanges of energy between pitch and roll-yaw with a period of about 30 orbits (Breakwell and Pringle, 1965:307). For a value of $r_o = 0.25$ and an elevator frequency of $w = n$, the chosen (r_1, r_2) combination that produced the internal resonance case results in a point "A" (See Fig. 18) within the unstable pitch zone of the Strutt diagram. To confirm this prediction, the elevator was turned on at $w = n$, and the unbounded pitch motion coupled energy into the roll and yaw axes to yield tumbling along all three axes.

V. Conclusions and Recommendations

Conclusions

This study has led to the following conslusions:

1. For the problem of a simple, gravity gradient stabilized, rigid body, the addition of elevators introduces time varying moments of inertia into the equations of motion.
2. For a single elevator mechanism whose travel along the yaw axis is described by a sinusoid, the resulting pitch motion is described by Hill's equation, in which the elevator acts as an energy source which creates an instance of parametric excitation.
3. The occasional traverse of the elevator from one end to the other does not cause the instability studied in this paper. Motion must be continuous over many periods.
4. Mathieu stability analysis for the linearized pitch equation yields an approximate lower bound of elevator frequency $w = 1.9n$ for stable, bounded pitch motion.
5. The Lagrange region of stability predicted by linear analysis as well as Liapunov's direct method (Hughes, 1986:294) for a gravity gradient stabilized rigid body may contain regions of instability when an elevator is operating along one of the principal axes. The existence of these unstable regions require that the elevator operating period be at or near the orbit period. The extent of the area of

parametric instability within the Lagrange region is determined by the ratio of the effective moment of inertia of the elevator to the pitch moment of inertia of the space station.

6. The results of numerical analysis show that the linearized analytical solution gives a fair approximation of the location of the 1st unstable region.

Recommendations

It is recommended that an analytical solution to the coupled roll-yaw equations be derived, from which a basis can be formed to predict the elevator effect in three dimensions. One can expect similar results in that further restrictions be placed within the Lagrange region. Also, it should be possible to control disturbance induced oscillations by making the elevator position proportional to the pitch angle instead of prescribing the elevator motion beforehand. Furthermore, the addition of the elevator problem might be considered in conjunction with the effects of flexibility on the stability of the space station.

Appendix A

Equations of Motion Using Euler Parameters

Time differentiation of the quaternion is described by

$$d/dt[\underline{q}] = (1/2)Z\underline{q} \tag{A-1}$$

(Wertz, 1980:512) where Z is the skew-symmetric matrix

$$Z = \begin{bmatrix} 0 & w_u & -w_v & w_u \\ -w_u & 0 & w_u & w_v \\ w_v & -w_u & 0 & w_u \\ -w_u & -w_v & -w_u & 0 \end{bmatrix} \tag{A-2}$$

and

$$\underline{q} = \begin{Bmatrix} q_1 \\ q_2 \\ q_3 \\ q_4 \end{Bmatrix} \tag{A-3}$$

and w_u, w_v, and w_u are the components of the angular velocity ${}^{o}\underline{w}^{B}$ expressed in the principal body basis. Since

$${}^{I}\underline{w}^{B} = {}^{I}\underline{w}^{O} + {}^{O}\underline{w}^{B} \tag{A-4}$$

Or,

$$\begin{Bmatrix} w_1 \\ w_2 \\ w_3 \end{Bmatrix} = \begin{Bmatrix} A_{13}n + w_u \\ A_{23}n + w_v \\ A_{33}n + w_w \end{Bmatrix} \tag{A-5}$$

Solve for w_u, w_v, and w_w, and substitute them into the expanded form of Eq (A-1)

$$\dot{q}_1 = (1/2)(q_2w_w - q_3w_v + q_4w_u) \tag{A-6a}$$

$$\dot{q}_2 = (1/2)(-q_1w_w + q_3w_u + q_4w_v) \tag{A-6b}$$

$$\dot{q}_3 = (1/2)(q_1w_v - q_2w_u + q_4w_w) \tag{A-6c}$$

$$\dot{q}_4 = (1/2)(-q_1w_u - q_2w_v - q_3w_w) \tag{A-6d}$$

And Eq (A-6) can be rewritten as

$$\dot{q}_1 = (1/2)[q_2(w_3 - A_{33}n) - q_2(w_2 - A_{23}n) + q_4(w_1 - A_{13}n)] \tag{A-7a}$$

$$\dot{q}_2 = (1/2)[-q_1(w_3 - A_{33}n) + q_3(w_1 - A_{13}n) + q_4(w_2 - A_{23}n)] \tag{A-7b}$$

$$\dot{q}_3 = (1/2)[q_1(w_2 - A_{23}n) - q_2(w_1 - A_{13}n) + q_4(w_3 - A_{33}n)] \tag{A-7c}$$

$$\dot{q}_4 = (1/2)[-q_1(w_1 - A_{13}n) - q_2(w_2 - A_{23}n) - q_3(w_3 - A_{33}n)] \tag{A-7d}$$

Eqs (A-7a) through (A-7d) are the equivalent set of kinematic equations to be used instead of Eqs (18). Also needed in addition to Eqs (A-7a) through (A-7d) to work with euler parameters are the following relations:

$$q_1 = (1/4q_4)(A_{23}-A_{32}) \qquad \text{(A-8a)}$$

$$q_2 = (1/4q_4)(A_{31}-A_{13}) \qquad \text{(A-8b)}$$

$$q_3 = (1/4q_4)(A_{12}-A_{21}) \qquad \text{(A-8c)}$$

$$q_4 = (1/2)(1+A_{11}+A_{22}+A_{33}+A_{44}) \qquad \text{(A-8d)}$$

which give euler parameters in terms of the elements of the direction cosine matrix A. Similarly, A in terms of $\underline{q}$ is seen to be

$$A(\underline{q}) = \begin{bmatrix} q_1^2-q_2^2-q_3^2+q_4^2 & 2(q_1q_2+q_3q_4) & 2(q_1q_3-q_2q_4) \\ 2(q_1q_2-q_3q_4) & -q_1^2+q_2^2-q_3^2+q_4^2 & 2(q_2q_3+q_1q_4) \\ 2(q_1q_3+q_2q_4) & 2(q_2q_3-q_1q_4) & -q_1^2-q_2^2+q_3^2+q_4^2 \end{bmatrix} \qquad \text{(A-9)}$$

Thus, all equations have been collected in order to work with euler parameters.

Appendix B

Expansion of Periodic Coefficient

Consider the dumbbell configuration in Fig. 1 in which the entire mass of the space station minus the elevator mass, m_e, is concentrated in two spheres of mass m_s, and the length of elevator travel along the $\hat{b}_1$ direction is L. The moments of inertia about the composite center of mass can be described by

$$I_1 = I_{o1} \tag{B-1a}$$

$$I_2 = I_{o2} + M[(L/2)\sin(wt)]^2 \tag{B-1b}$$

$$I_3 = I_{o3} + M[(L/2)\sin(wt)]^2 \tag{B-1c}$$

where $M = [m_e m_s/(m_e+m_s)]$ is the "reduced" mass of the elevator, and I_{o1}, I_{o2}, and I_{o3} are the principal moments of inertia about the center of mass for a space station without the elevator mechanism. A time derivative of Eq (B-1b) yields

$$\dot{I} = \dot{I}_2 = \dot{I}_3 = [wML^2\sin(wt)\cos(wt)]/2 \tag{B-2}$$

Inserting Eq (B-2) into Eq (36) gives the result

$$P(t) = \left[\frac{1 \;\; (1/2)wML^2\sin(wt)\cos(wt)}{2 \;\; I_{o3}+M[(L/2)\sin(wt)]^2}\right] \tag{B-3}$$

Squaring Eq (B-3) yields

$$P^2(t) = \frac{1}{4}\left[\frac{(1/4)w^2M^2L^4\sin^2(wt)\cos^2(wt)}{\langle I_{o3}+M[(L/2)\sin(wt)]^2\rangle^2}\right] \qquad (B\text{-}4)$$

Taking a time derivative of Eq (B-3) yields

$$\dot{P}(t) = (wML^2/4)[wC\cos^2(wt)-wC\sin^2(wt) - (1/2)C^2\sin^2(wt)\cos^2(wt)] \qquad (B\text{-}5)$$

where $C = [I_{o2} + (1/4)ML^2\sin^2(wt)]^{-1}$.

Now, insert Eqs (B-1a), (B-1b), and (B-1c) into Eq (37) and get the result

$$R^2(t) = 3n^2C[I_{o2}+(1/4)ML^2\sin^2(wt)-I_{o1}] \qquad (B\text{-}6)$$

Collect all terms, P^2, $\dot{P}$, and R^2, from Eqs (B-4), (B-5), and (B-6), respectively, and plug them into the transformed pitch equation, Eq (44):

$$\ddot{y} + \{3n^2C[I_{o2}+(1/4)ML^2\sin^2(wt)-I_{o1}] - (1/16)C^2w^2M^2L^4\sin^2(wt)\cos^2(wt) - (1/4)wML^2[Cw\cos^2(wt) - Cw\sin^2(wt) - (1/2)C^2wML^2\sin^2(wt)\cos^2(wt)]\}\, y = Q\exp[\int P\,dt] \qquad (B\text{-}7)$$

Notice the often occuring term

$$C = [I_{o3}+(1/4)ML^2\sin^2(wt)]^{-1} \qquad (B\text{-}8)$$
$$= (1/I_{o3})(1 + x)^{-1}$$

where $x = r_o\sin^2(wt)$ and $r_o = ML^2/4I_{o3}$.

C can be expanded using the binomial series

$$(1+x)^{-1} = 1 - x + x^2 - x^3 + ... \qquad (B\text{-}9)$$

Similarly, the term

$$C^2 = (1/I_{o3}^2)(1+x)^{-2} \qquad (B\text{-}10)$$

can be expanded using

$$(1+x)^{-2} = 1 - 2x + 3x^2 - 4x^3 + ... \qquad (B\text{-}11)$$

Now, to decide how many terms will approximate each series, consider the following: To determine r_o and I_{o3}, recall how the entire mass of the rigid space station without the elevator was concentrated in two spheres of mass m_s. Consequently, $I_{o3} = (1/2)m_sL^2$ and $r_o = (1/2)(M/m_s)$. (This is valid since gravity gradient stabilization depends on ratios of inertias and not actual magnitudes, and ratios are what are being expressed here.) Reasonable elevator masses

set a maximum $r_o = 1/4$, which corresponds to $m_E = m_s$. Also, performing a few simple calculations shows that approximating $(1+x)^{-1}$ and $(1+x)^{-2}$ with three terms yields an inconsequential error while keeping the number of terms in the approximation to a minimum. Hence, insert three term series' into Eq (B-7) and obtain

$$\ddot{z} + \left\{(3n^2/I_{o3})[I_{o2}+(1/4)ML^2\sin^2(wt)-I_{o1}](1-x+x^2) - A'(1-2x+3x^2) - B'C'(1-x+x^2) + B'D'(1-2x+3x^2)\right\} z = 0 \quad \text{(B-12)}$$

where the homogeneous equation is being analyzed and the terms A', B', C', and D' are given by

$$A' = (w^2M^2L^4/16I_{o3}^2)\sin^2(wt)\cos^2(wt)$$
$$= w^2r_o^2\sin^2(wt)\cos^2(wt)$$
$$B' = (w^2ML^2/4I_{o3})$$
$$C' = w[\cos^2(wt)-\sin^2(wt)]$$
$$D' = (wML^2/2I_{o2}^2)\sin^2(wt)\cos^2(wt)$$

B'C' and B'D' simplifies to

$$B'C' = w^2r_o\cos(2wt)$$
$$B'D' = 2w^2r_o^2\sin^2(wt)\cos^2(wt)$$

Insert expressions for B'C' and B'D' into Eq (B-12), carry out the various multiplications, and obtain the result

$$\ddot{z} + \{3n^2r_2 + 3n^2r_o\sin^2(wt) - 3n^2r_1 - 3n^2r_2(x) - 3n^2r_o\sin^2(wt)(x) + 3n^2r_1(x) + 3n^2r_2(x^2) + 3n^2r_o\sin^2(wt)(x^2) - 3n^2r_1(x^2) - A' + 2A'x - 3A'x^2 - B'C' + B'C'x - B'C'x^2 + B'D' - 2B'D'x + 3B'D'x^2\} z = 0 \quad (B\text{-}13)$$

Or,

$$\ddot{z} + \{3n^2r_2 + 3n^2r_o\sin^2(wt) - 3n^2r_1 - 3n^2r_2r_o\sin^2(wt) - 3n^2r_o^2\sin^4(wt) + 3n^2r_1r_o\sin^2(wt) + 3n^2r_2r_o^2\sin^4(wt) + 3n^2r_o^3\sin^6(wt) - 3n^2r_1r_o^2\sin^4(wt) - w^2r_o^2\sin^2(wt)\cos^2(wt) + 2w^2r_o^3\sin^4(wt)\cos^2(wt) - 3w^2r_o^4\sin^6(wt)\cos^2(wt) - w^2r_o\cos(2wt) + w^2r_o^2\cos(2wt)\sin^2(wt) - w^2r_o^3\cos(2wt)\sin^4(wt) + 2w^2r_o^2 - 4w^2r_o^3\sin^2(wt) + 6w^2r_o^4\sin^4(wt)\} z = 0 \quad (B\text{-}14)$$

Note these trigonometric identities, and insert them into Eq (B-14):

$$\sin^2(wt) = 1/2 - (1/2)\cos(2wt)$$

$$\sin^4(wt) = 3/8 - (1/2)\cos(2wt) + (1/8)\cos(4wt)$$

$$\sin^6(wt) = (9/16)\sin^2(wt) - (3/16)\cos(2wt) + (3/16)\cos(4wt) - (1/32)\cos(6wt) + 1/32$$

$$\cos^2(wt) - \sin^2(wt) = \cos(2wt)$$

$$\cos^2(wt)\sin^2(wt) = 1/8 - (1/8)\cos(4wt)$$

$$\cos^2(wt)\sin^4(wt) = 1/16 - (1/32)\cos(2wt) - (1/16)\cos(4wt) + (1/32)\cos(6wt)$$

$$\cos^2(wt)\sin^6(wt) = 5/128 - (1/32)\cos(2wt) - (1/32)\cos(4wt) - (1/32)\cos(6wt) - (1/128)\cos(8wt)$$

$$\sin^2(wt)\cos(2wt) = -1/4 + (1/2)\cos(2wt) - (1/4)\cos(4wt)$$

Eq (B-15) then becomes

$$\ddot{z} + \Big\{3n^2r_2 + [1/2-(1/2)\cos(2wt)][3n^2r_o - 3n^2r_2r_o + 3n^2r_1r_o - 4w^2r_o^3] - 3n^2r_1 + [-3n^2r_o^2 + 3n^2r_o^2(r_2 - r_1) + 6w^2r_o^4][3/8 - (1/2)\cos(2wt) + (1/8)\cos(4wt)] + 3n^2r_o^3[9/32 - (9/32)\cos(2wt) - (3/16)\cos(2wt) + (3/16)\cos(4wt) - (1/32)\cos(6wt) + 1/32] - w^2r_o^2[1/8 - (1/8)\cos(4wt)] + 2w^2r_o^3[1/16 - (1/32)\cos(2wt) - (1/16)\cos(4wt) + (1/32)\cos(6wt) - 3w^2r_o^4[5/128 - (1/32)\cos(2wt) - (1/32)\cos(4wt) - (1/32)\cos(6wt) - (1/128)\cos(8wt)] - w^2r_o\cos(2wt) + w^2r_o^2[(1/2)\cos(2wt) - (1/4) - (1/4)\cos(4wt)] - w^2r_o^3[(3/8)\cos(2wt) - (1/4) - (1/4)\cos(4wt) + (1/16)\cos(2wt) + (1/16)\cos(6wt)] + 2w^2r_o^2\Big\} z = 0 \quad \text{(B-15)}$$

Group like terms of cos(2wt), cos(4wt), cos(6wt), and cos(8wt), and Eq (B-16) can be rewritten as

$$d^2z/dT^2 + [a_T + 16q_1\cos(2T) + 16q_2\cos(4T) + 16q_3\cos(6T) + 16q_4\cos(8T)]z = 0 \quad \text{(B-16)}$$

in which the independent variable has been changed from t to T through the definition $T = wt$, and the variables a_T, q_1, q_2, q_3, and q_4 are given by

$$a_T = (n/w)^2[r_2-r_1+(r_o/2)] + (3/2)(n/w)^2 r_o(r_1-r_2) + (9/8)(n/w)^2 r_o^2(r_2-r_1-1) + (13/8)r_o^2 - (13/8)r_o^3 + (273/128)r_o^4 + (15/16)(n/w)^2 r_o^3 \quad \text{(B-17)}$$

$$q_1 = (1/16)[(-3/2)(n/w)^2 r_o^2(r_2-r_1) + (3/2)(n/w)^2 r_o(r_2-r_1) - (45/32)(n/w)^2 r_o^3 + (3/2)(n/w)^2 r_o^2 - (3/2)(n/w)^2 r_o - (93/32)r_o^4 + (3/2)r_o^3 + r_o^2/2 - r_o] \quad \text{(B-18)}$$

$$q_2 = (1/16)[(3/8)(n/w)^2 r_o^2(r_2-r_1-1) + (27/32)r_o^4 + (9/16)(n/w)^2 r_o^3 - (1/8)(r_o^2 + (1/8)r_o^3] \quad \text{(B-19)}$$

$$q_3 = (1/16)[(-3/32)(n/w)^2 r_o^3 + (3/32)r_o^4] \quad \text{(B-20)}$$

$$q_4 = (3/2048)r_o^4 \quad \text{(B-21)}$$

Appendix C

Appendix C contains the Figures 1 through 22.

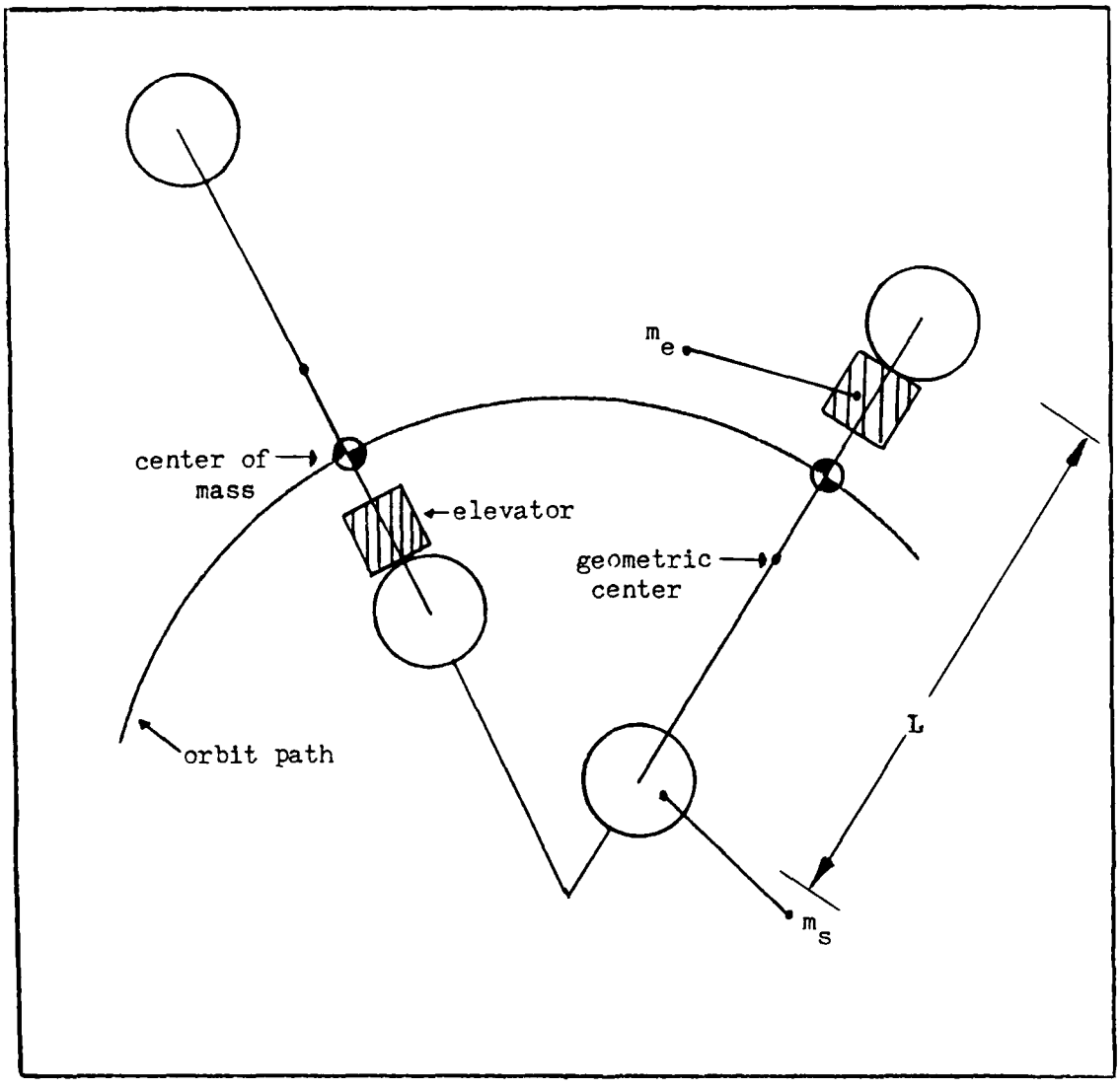

Fig. 1

Center of Mass

Dumbbell Configuration

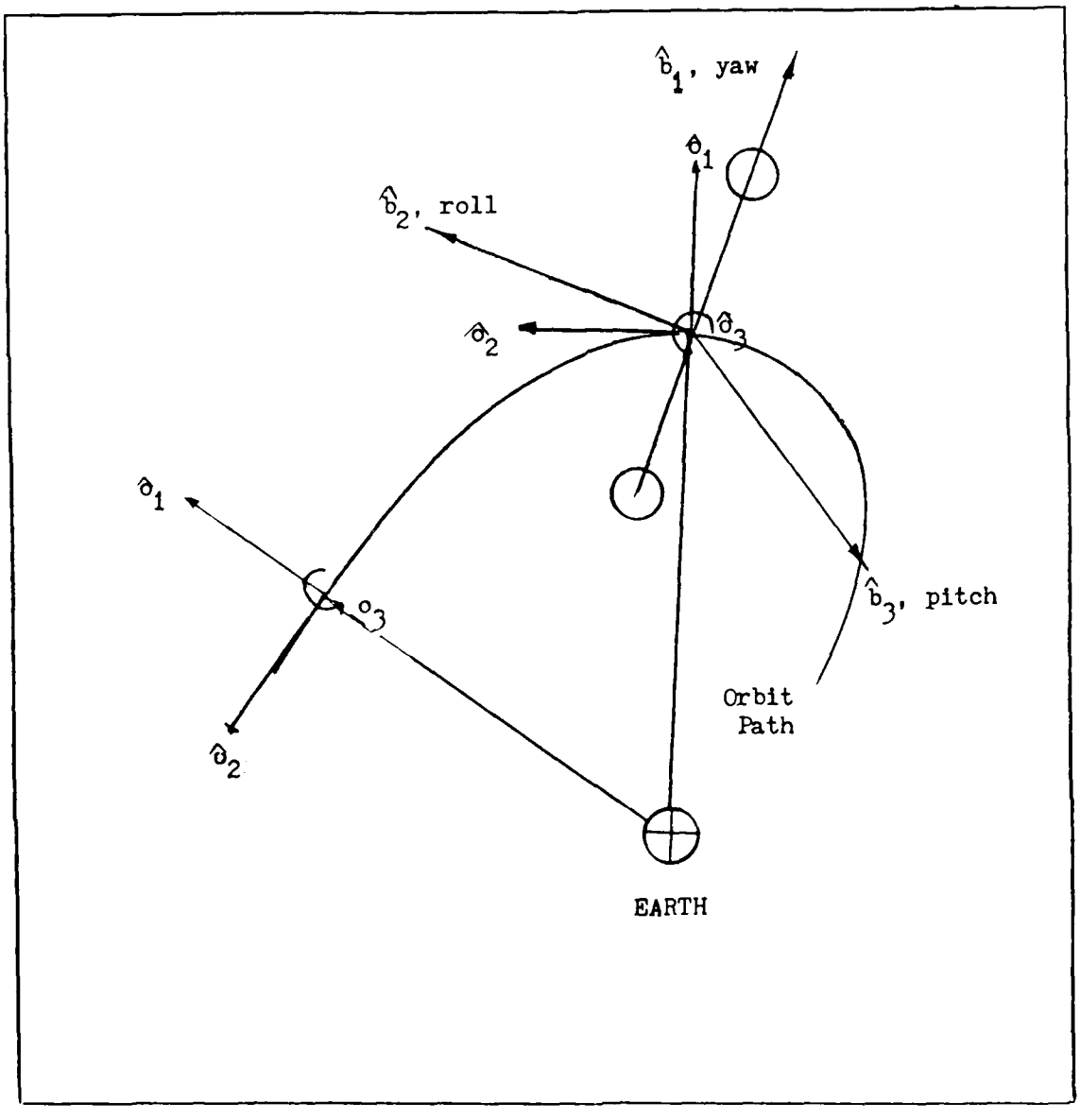

Fig. 2

Orbit & Body Axes

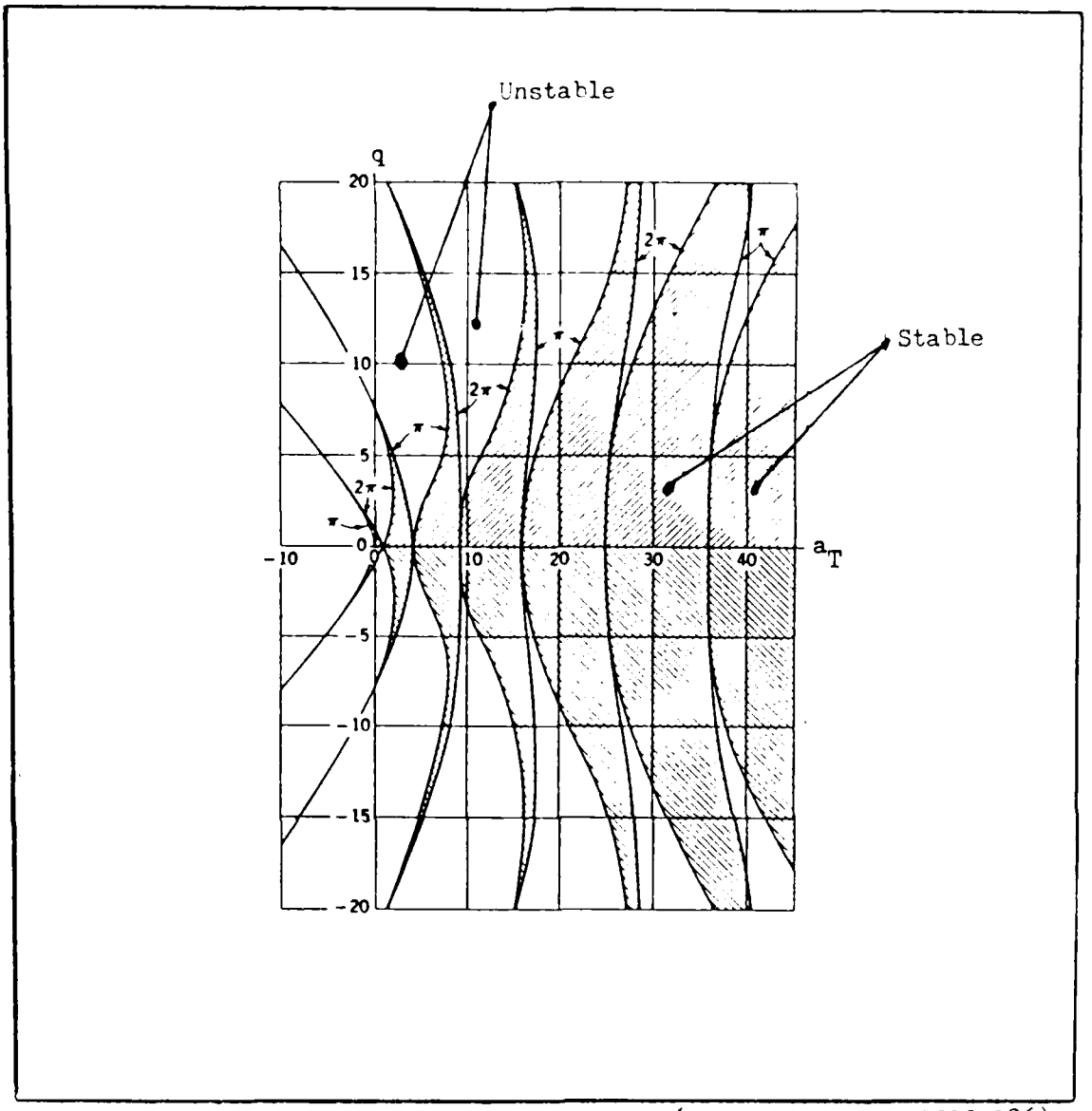

(Meirovitch, L., 1970:286)

Fig. 3

Strutt Diagram

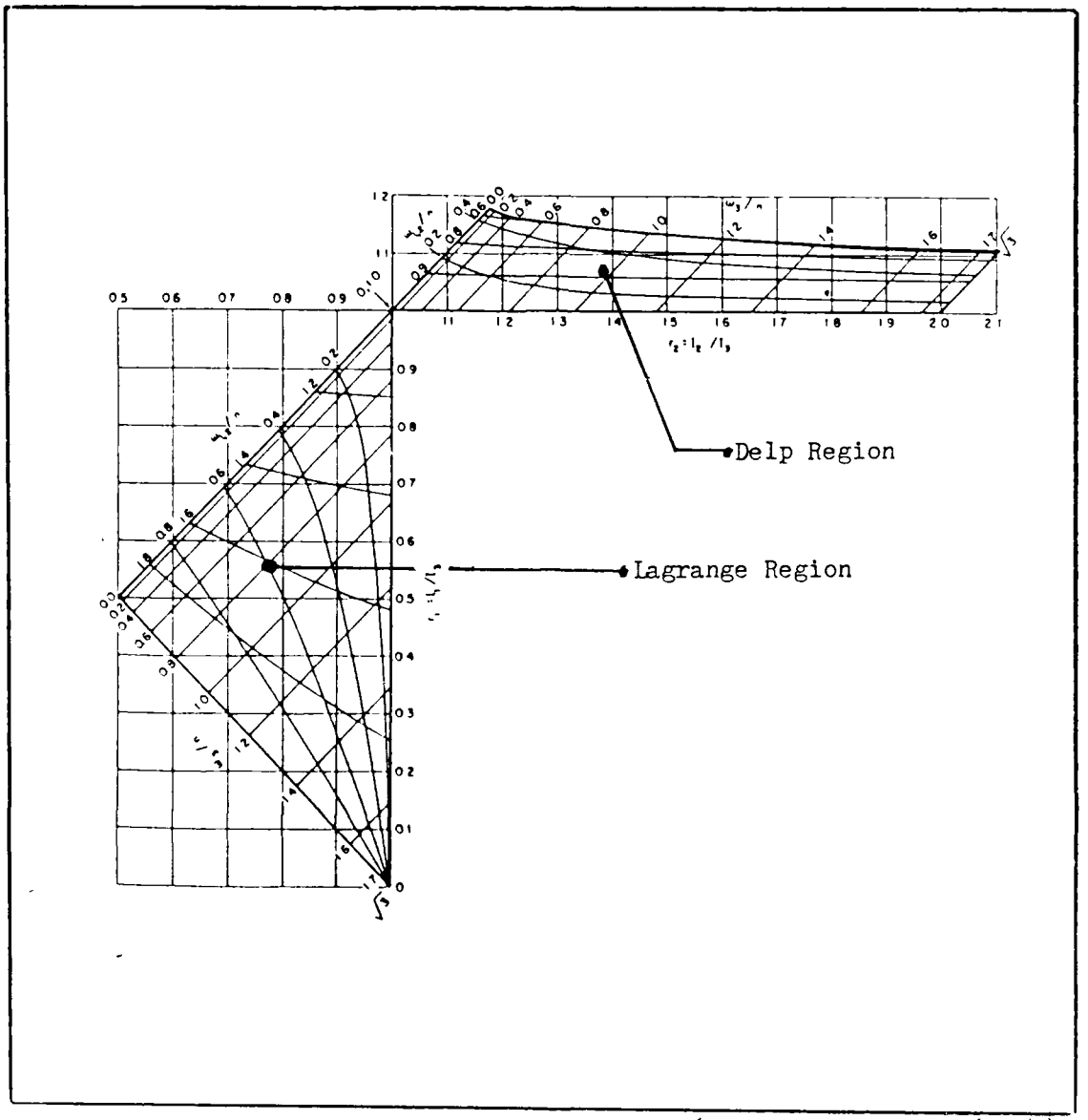

(Debra and Delp, 1961:14)

Fig. 4

Attitude Stability and Natural Frequencies of a Rigid Body in a Circular Orbit Plotted Versus r_1 and r_2

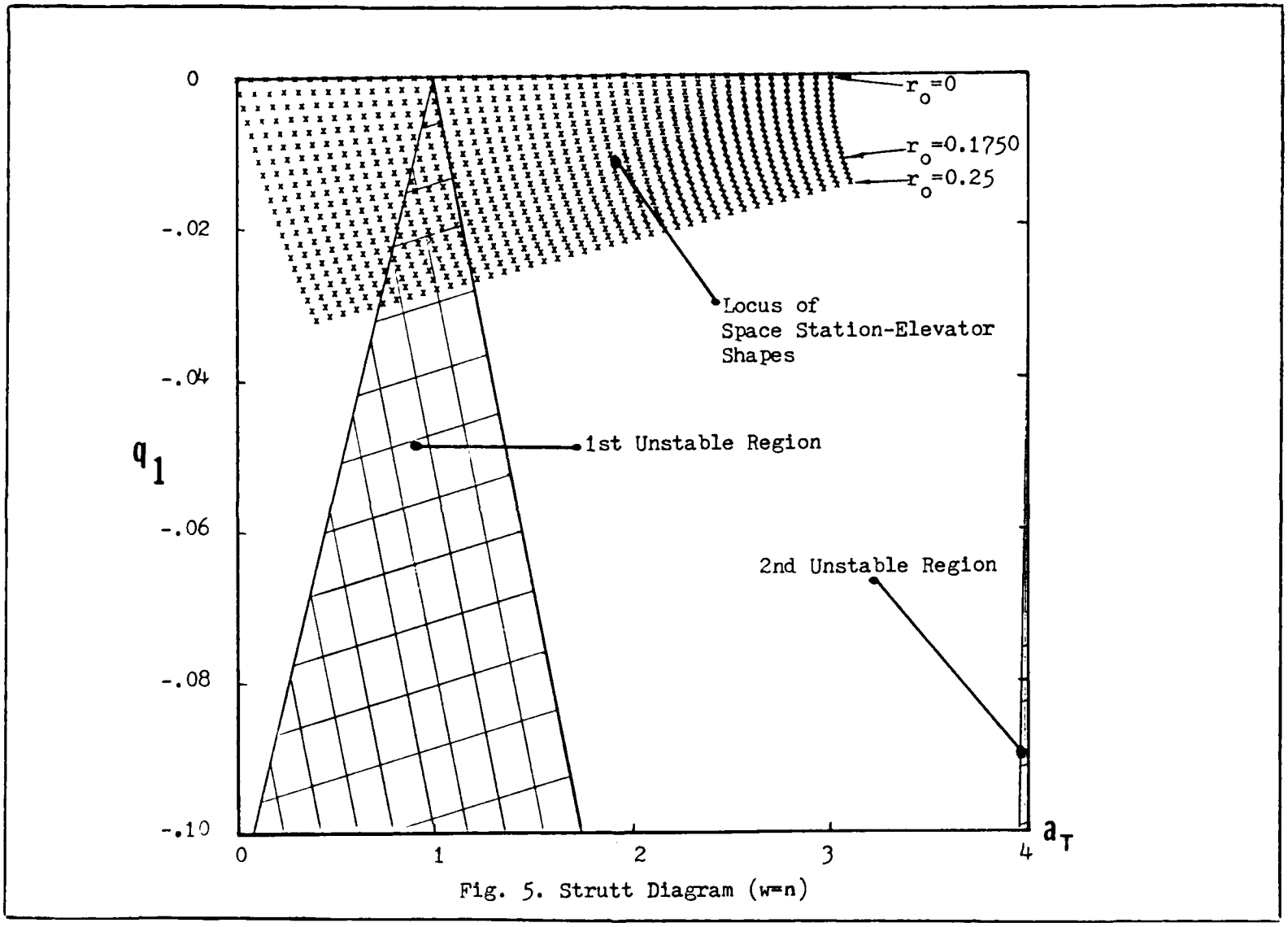

Fig. 5. Strutt Diagram (w=n)

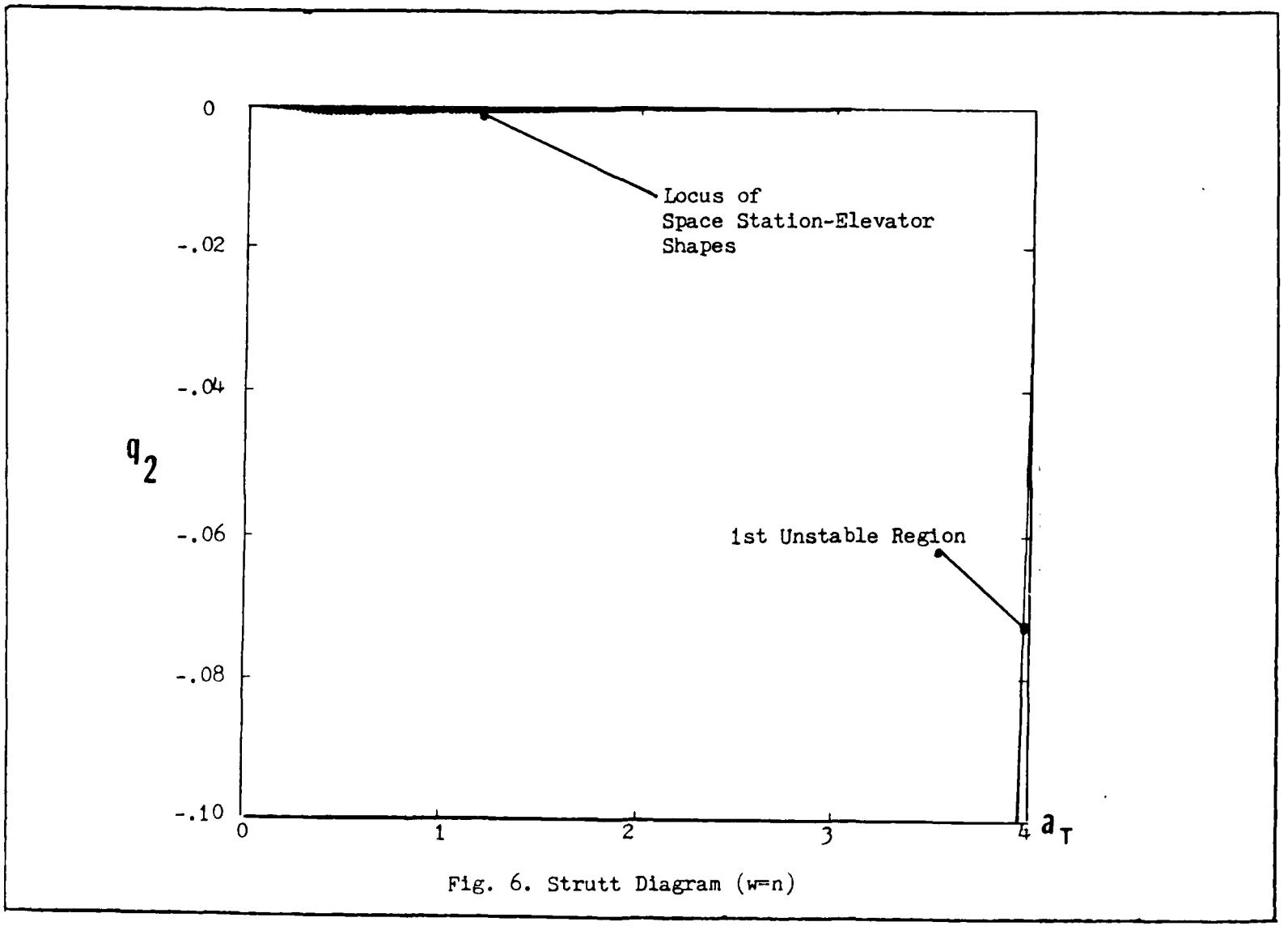

Fig. 6. Strutt Diagram (w=n)

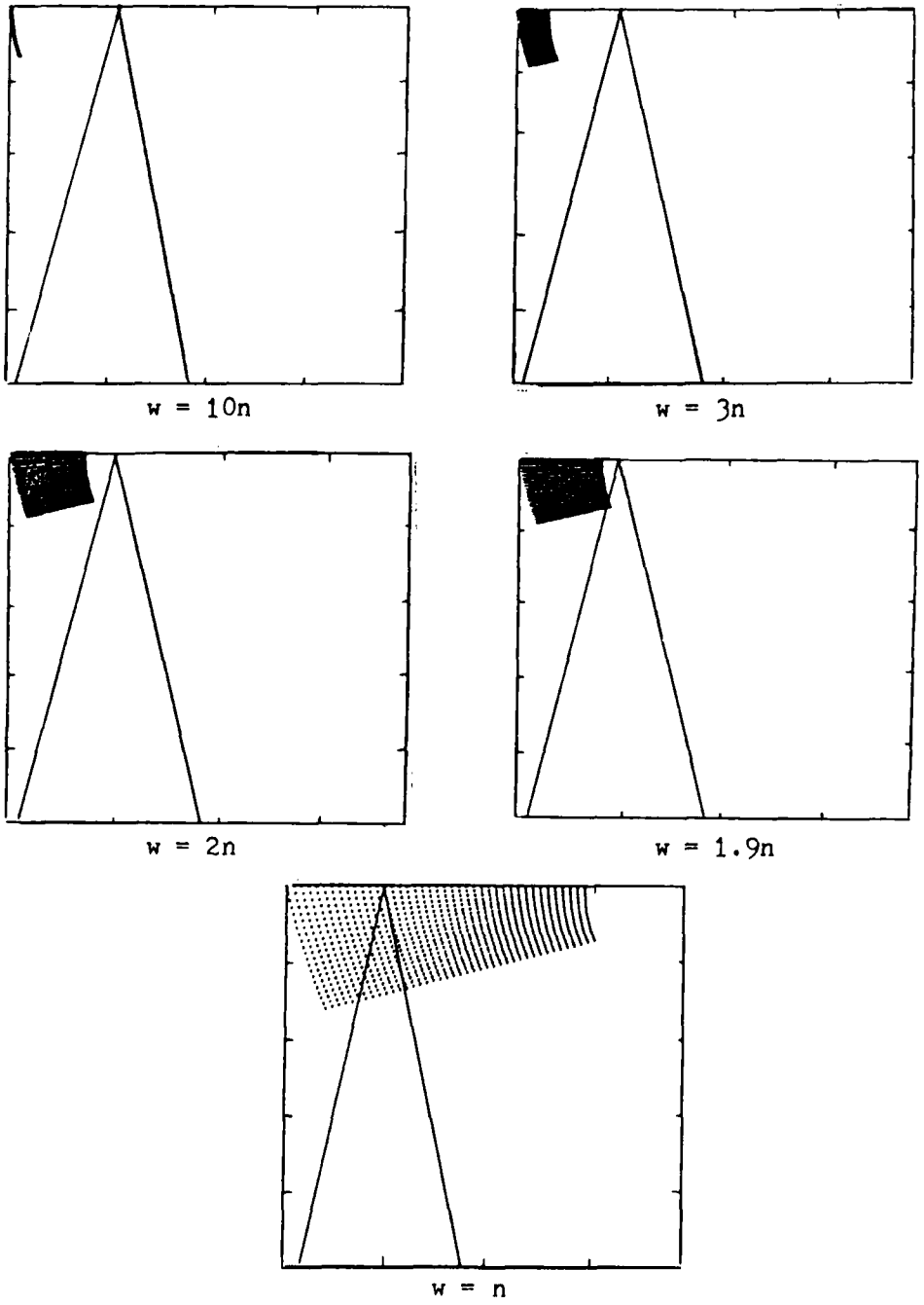

Fig. 7.
Effect of Changing Elevator Frequency, w,

on Locus of Space Station-Elevator Points

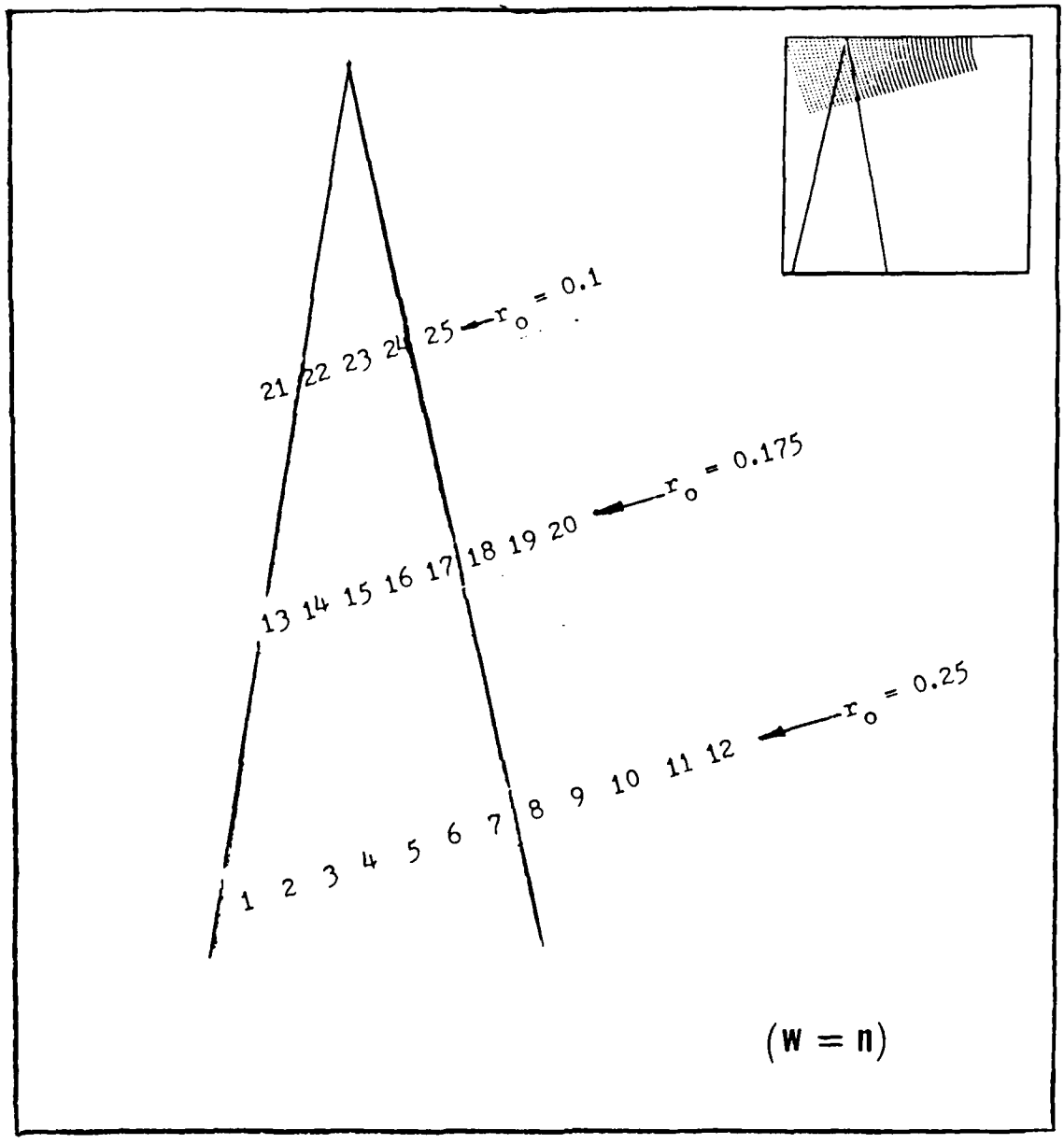

Fig. 8.

Enlargement - Prediction of Stable and Unstable Points

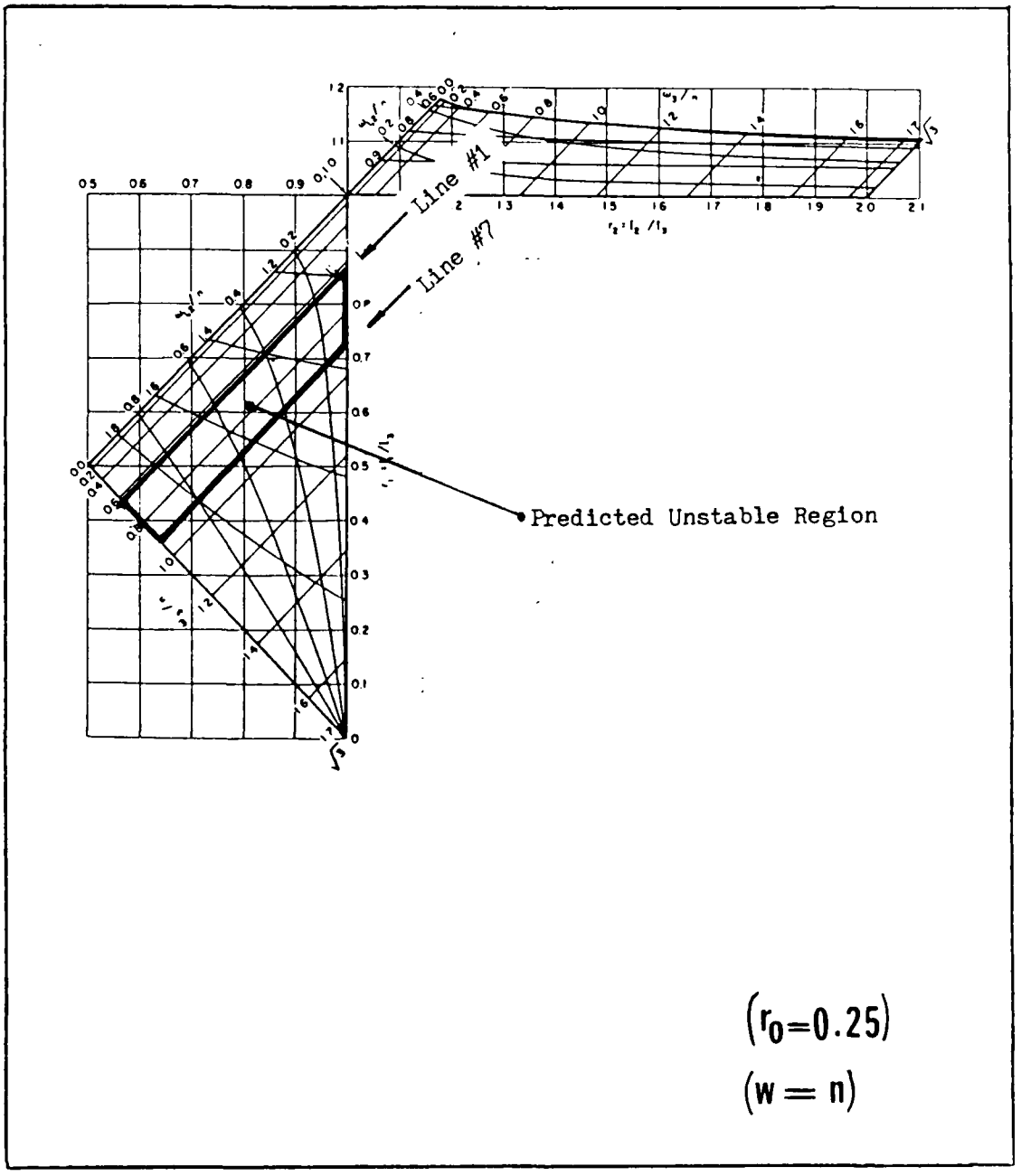

Fig. 9.

r_1-r_2 Mapping - Predicted Unstable Region

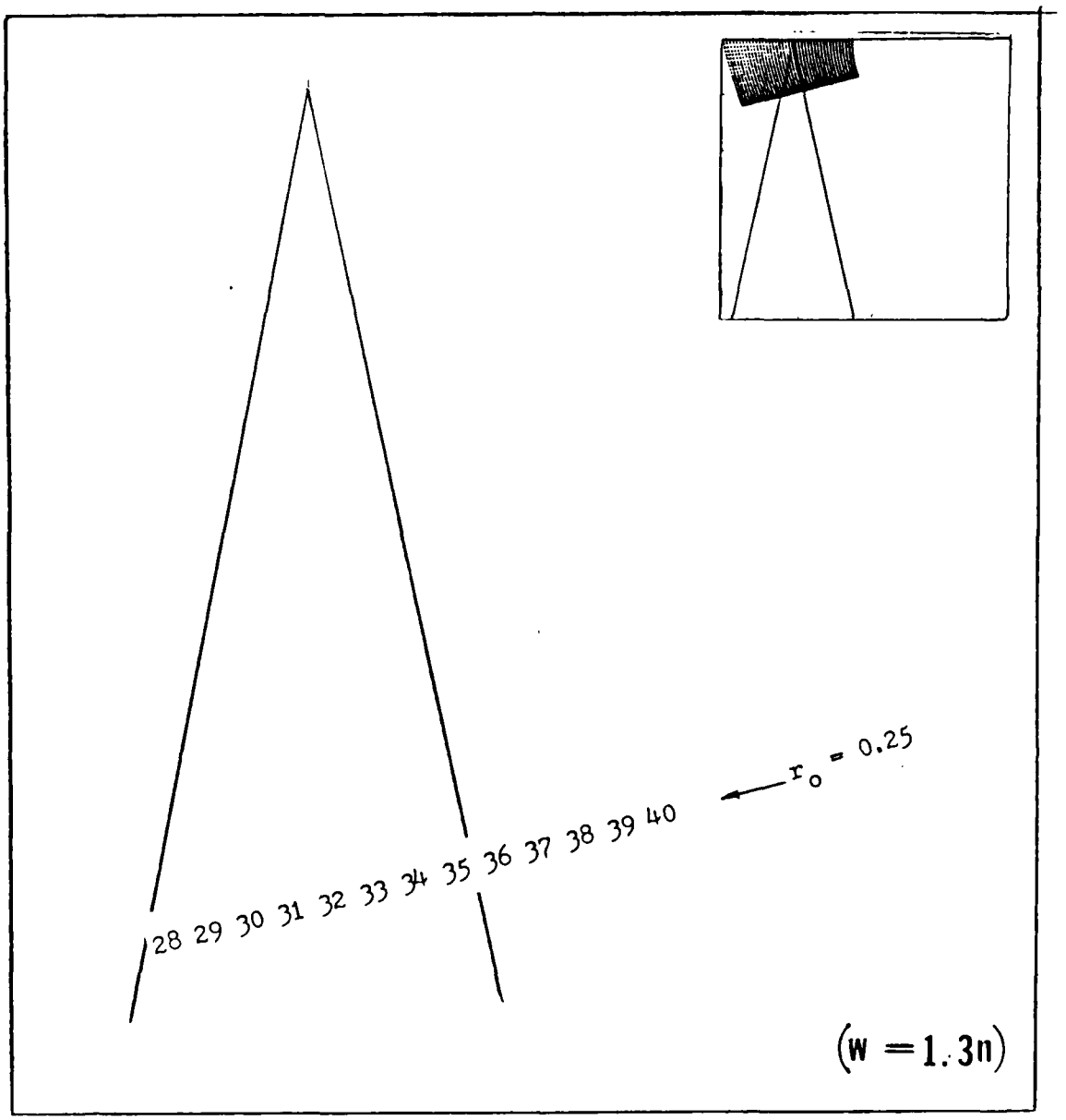

Fig. 10

Enlargement - Prediction of Stable and Unstable Points

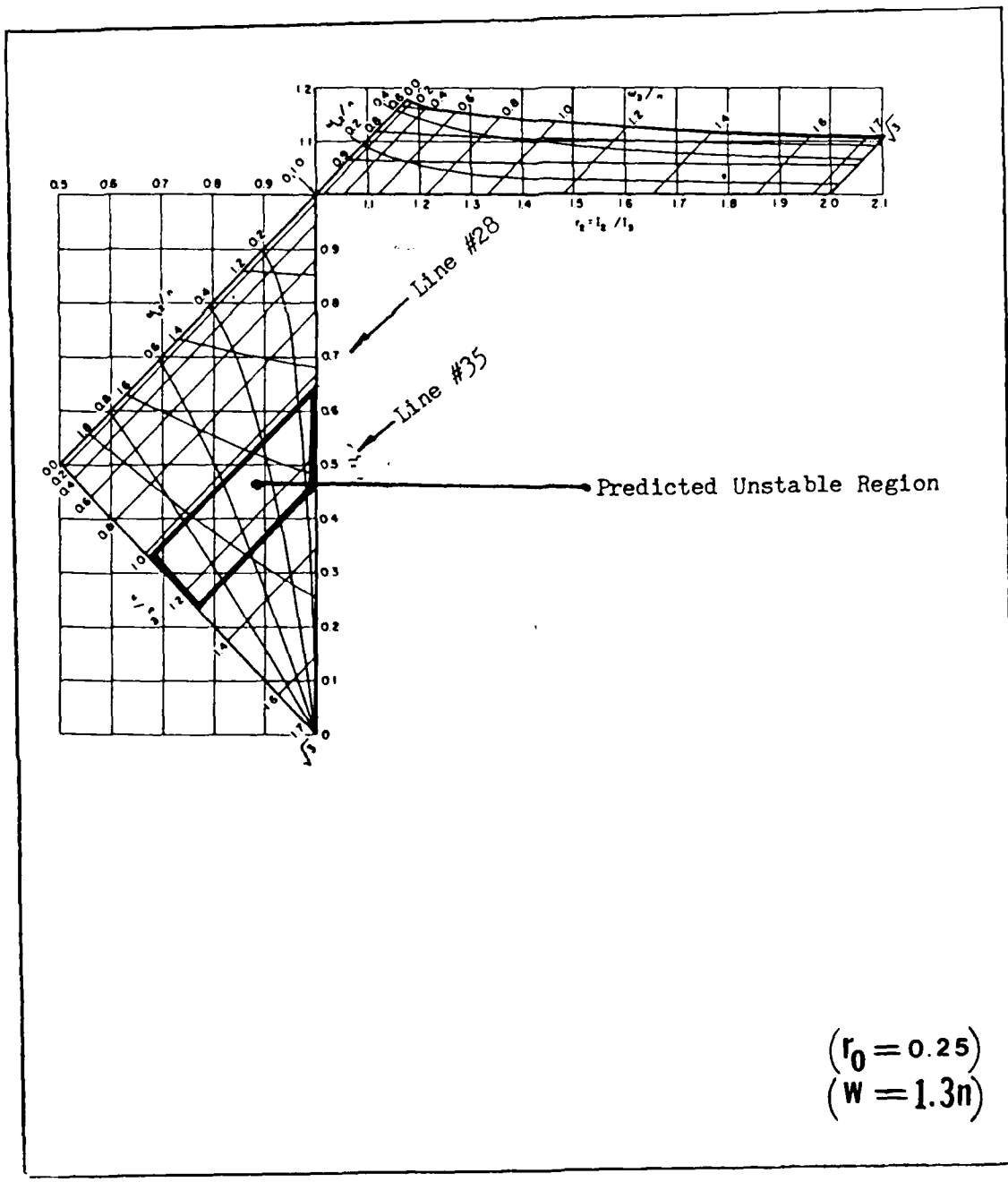

Fig. 11

r_1-r_2 Mapping - Predicted Unstable Region

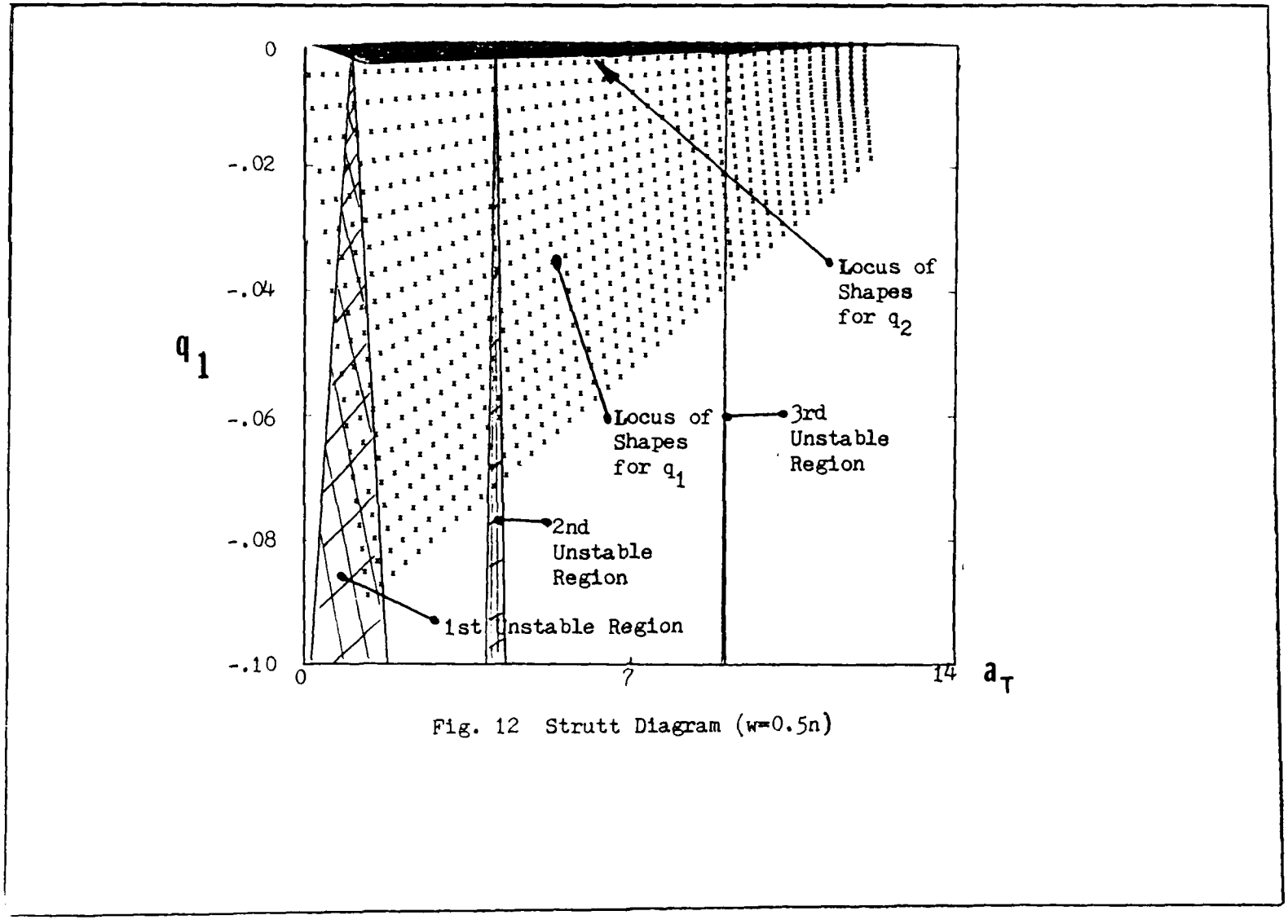

Fig. 12 Strutt Diagram (w=0.5n)

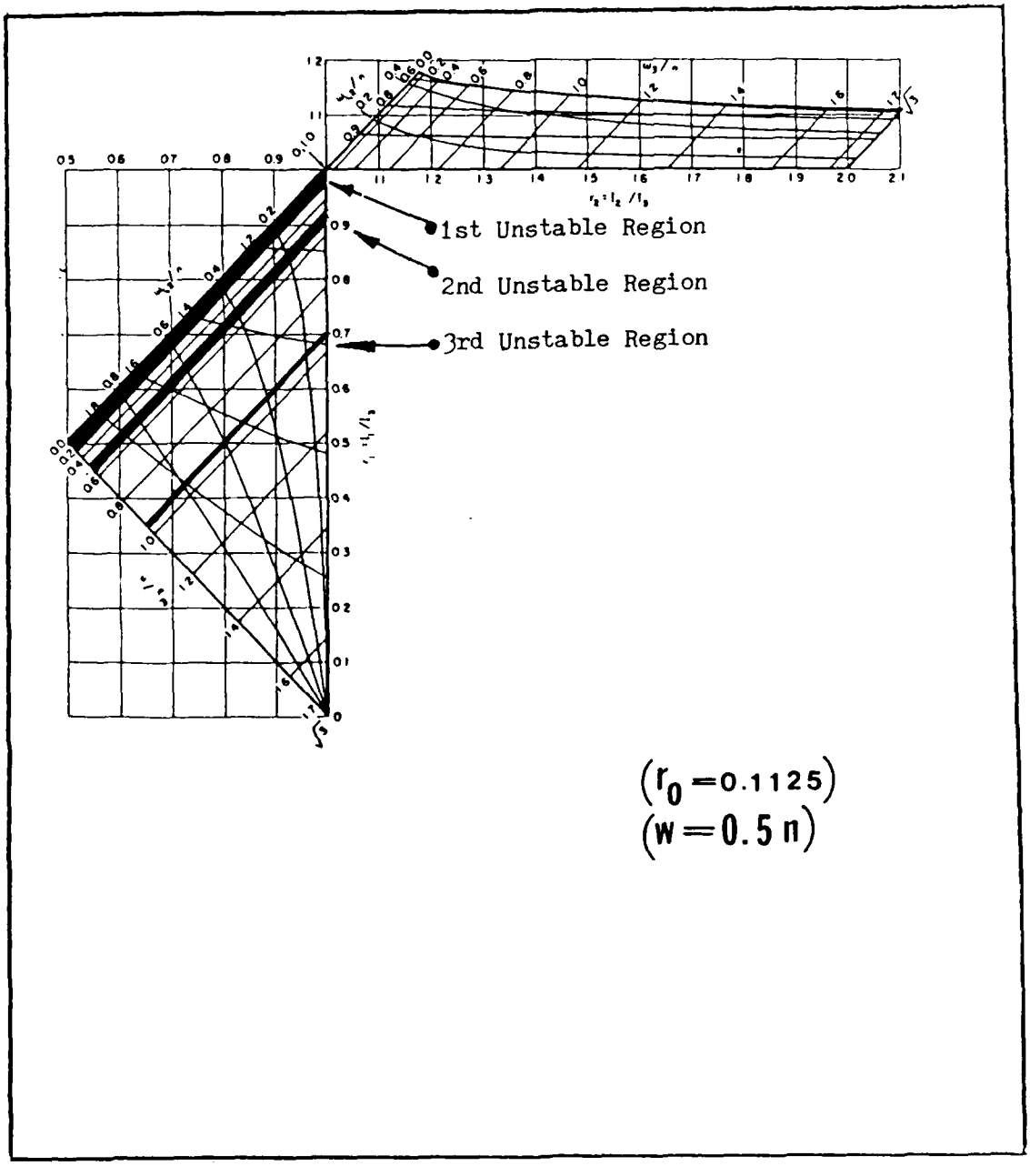

Fig. 13
Multiple Regions

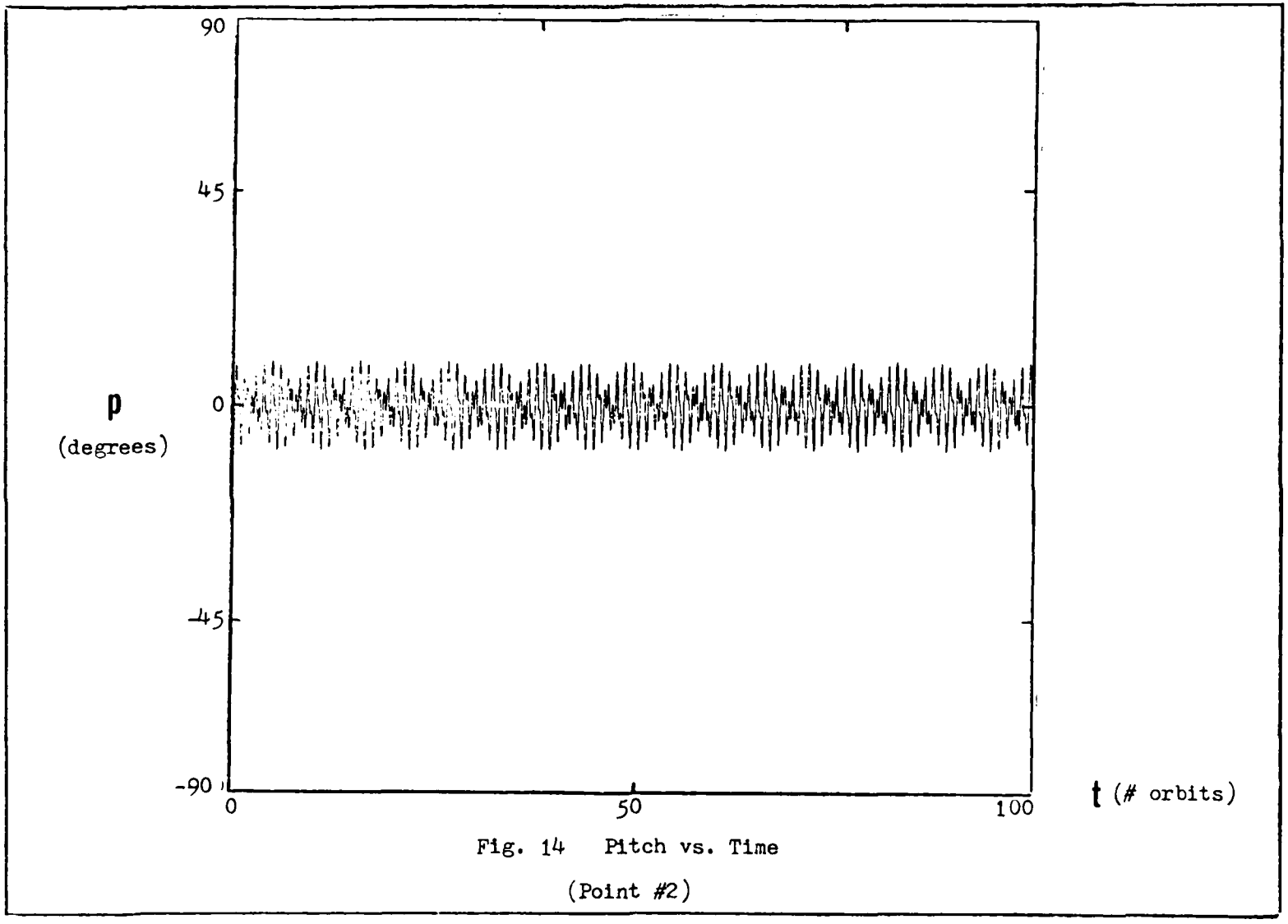

Fig. 14 Pitch vs. Time

(Point #2)

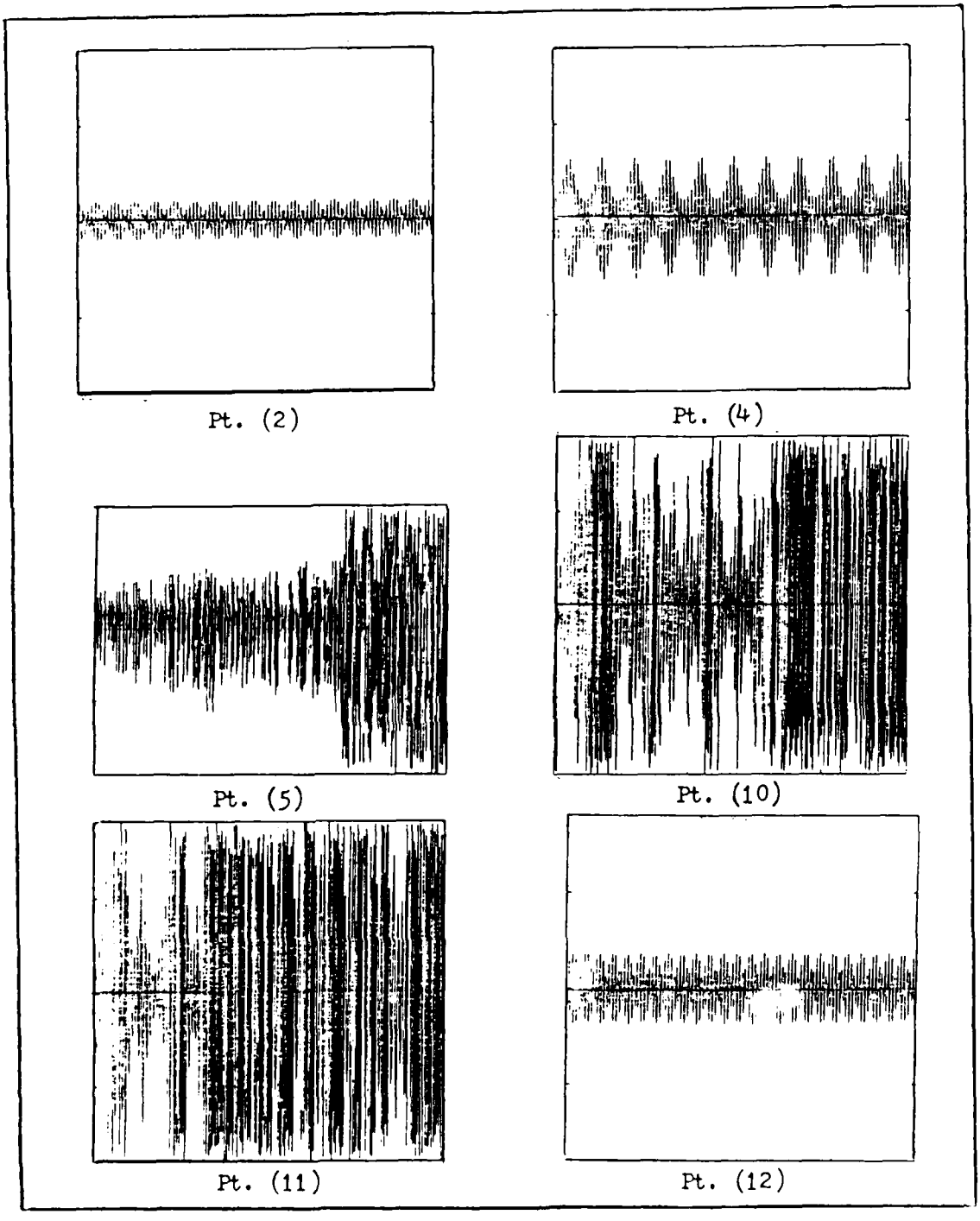

Fig. 15

Computer Runs ($w = n$, $r_o = 0.25$)

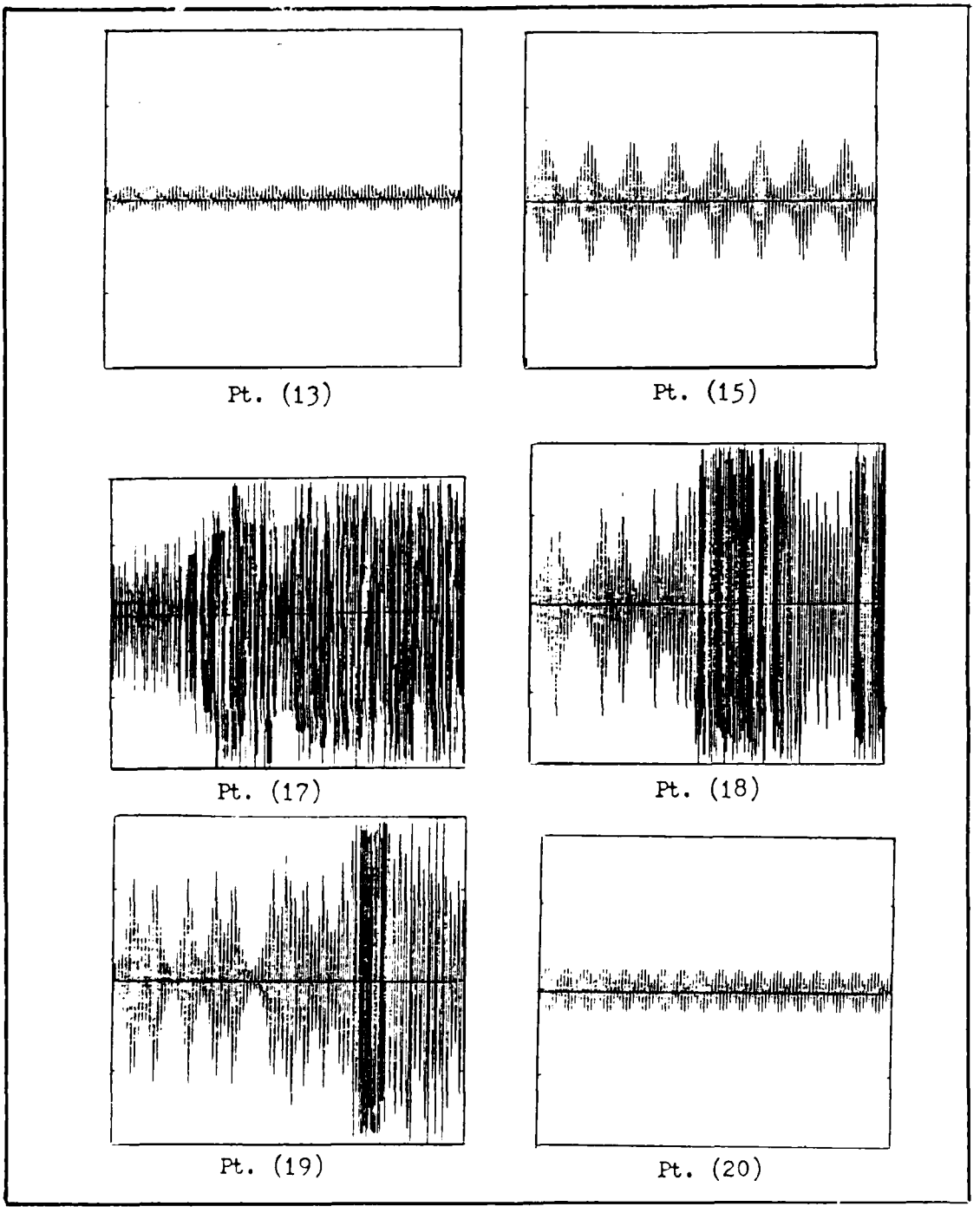

Fig. 16

Computer Runs ($w = n$, $r_o = 0.1750$)

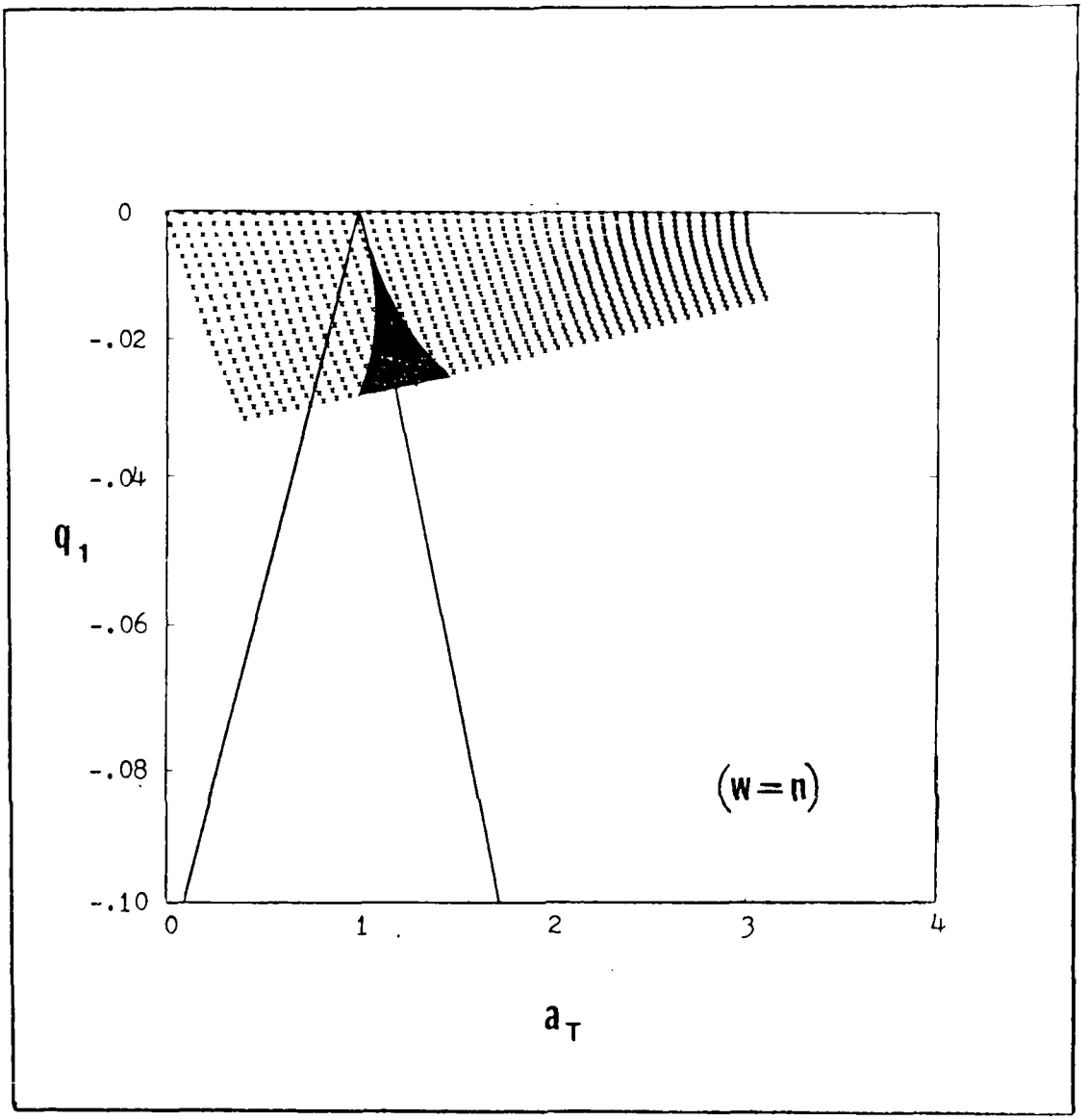

Fig. 17

Unstable Region - Numerical Solution

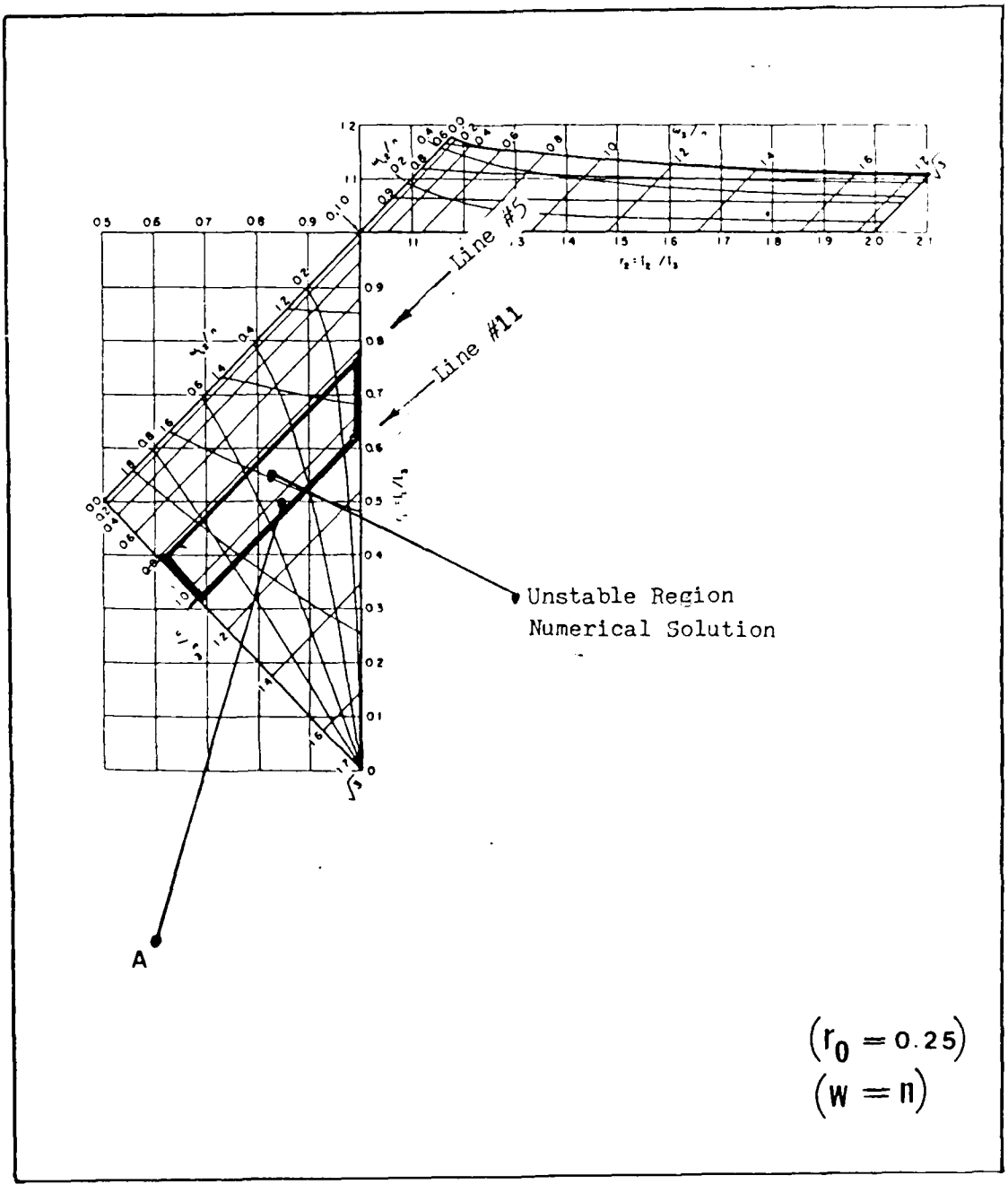

Fig. 18

r_1-r_2 Mapping - Numerical Solution

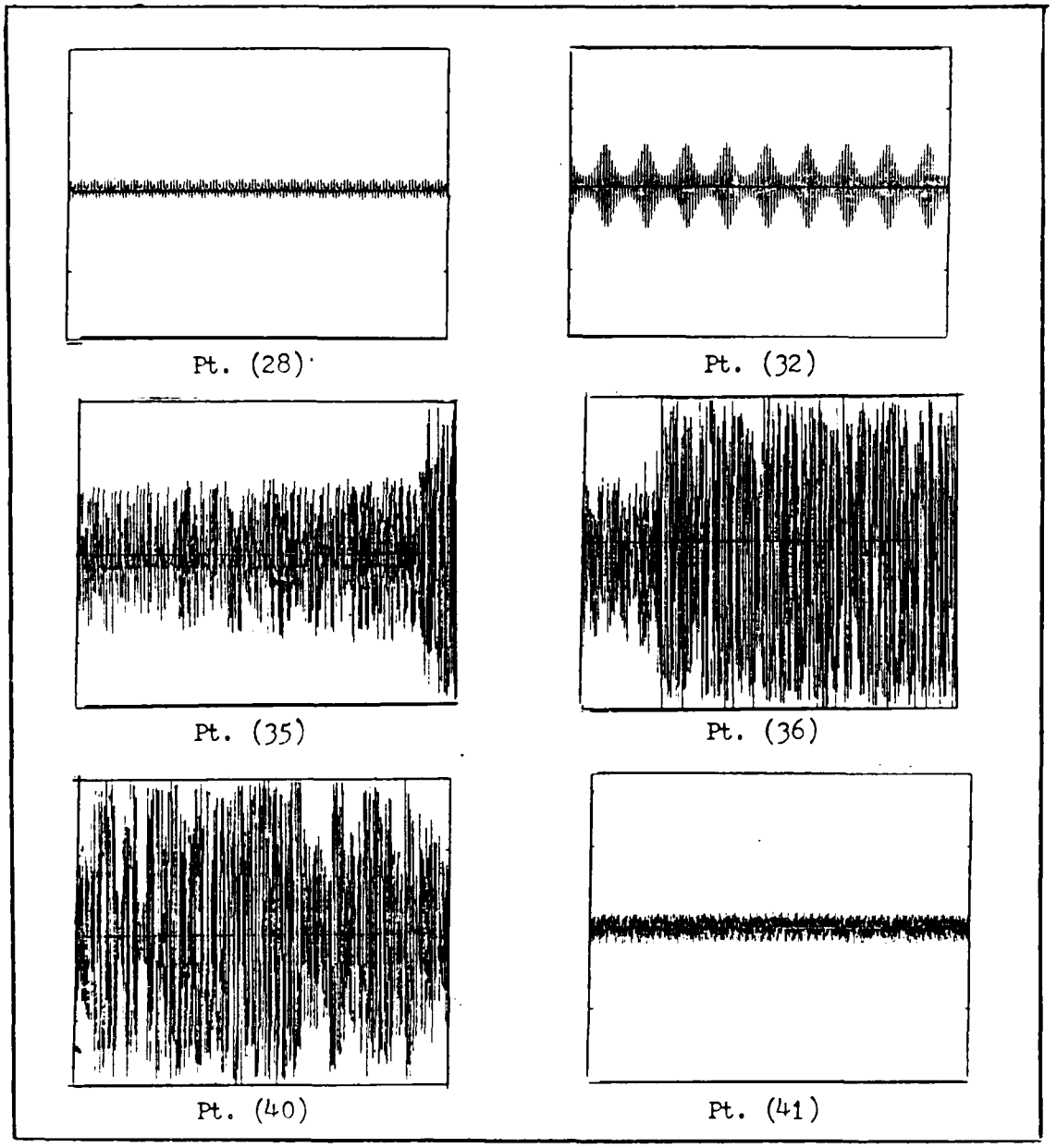

Fig. 19

Computer Runs ($w = 1.3n$, $r_o = 0.25$)

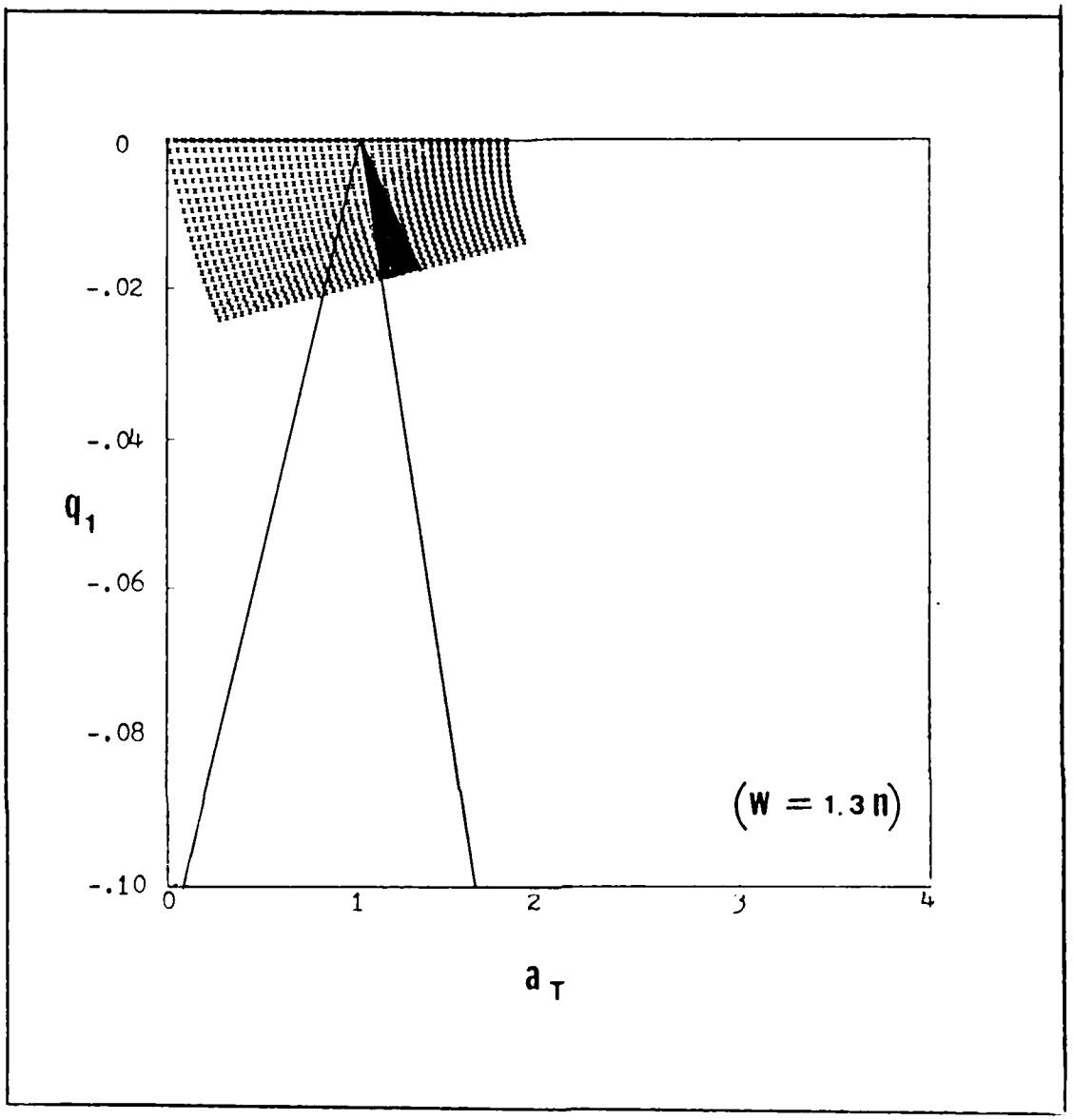

Fig. 20

Unstable Region - Numerical Solution

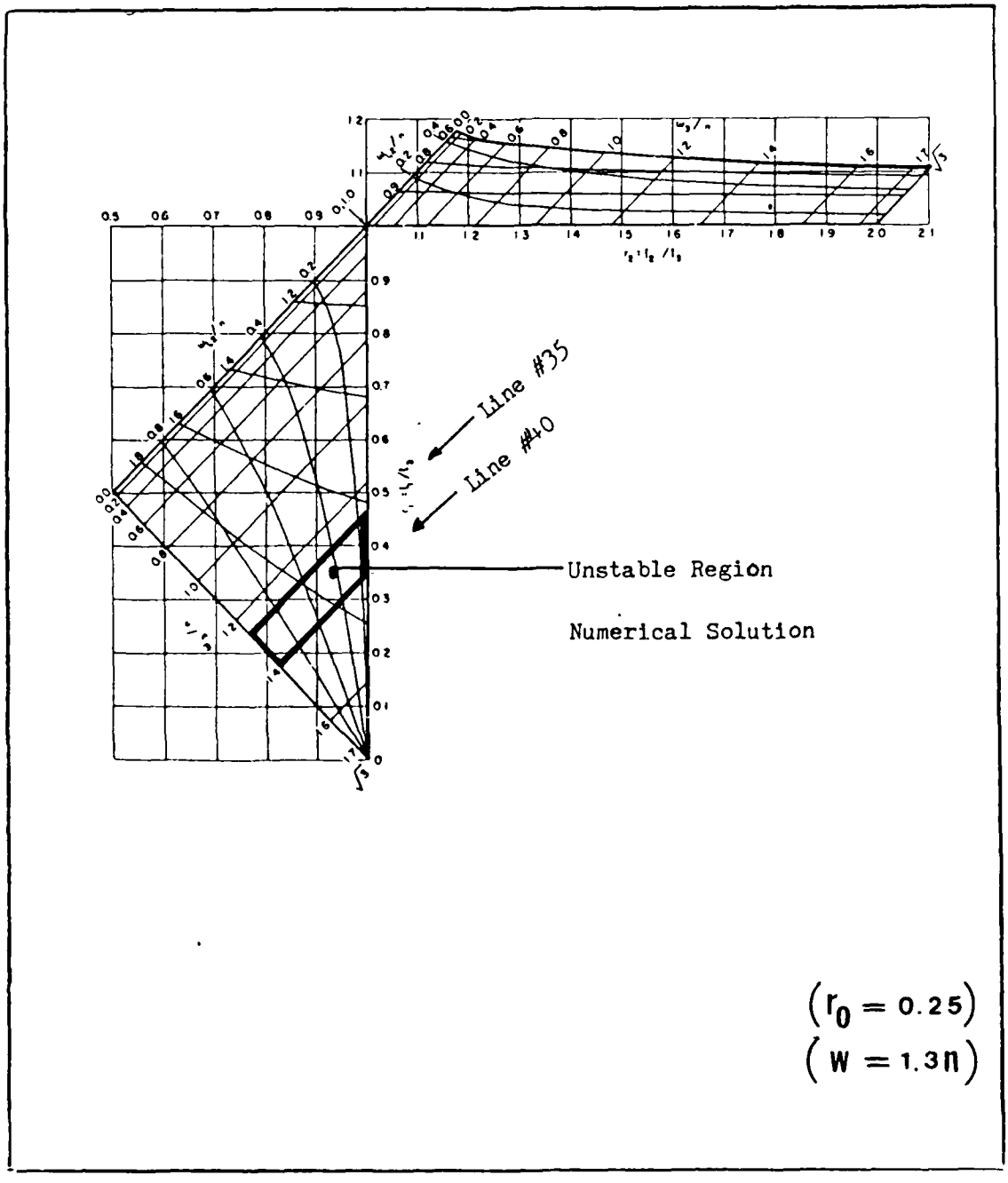

Fig. 21

r_1-r_2 Mapping - Numerical Solution

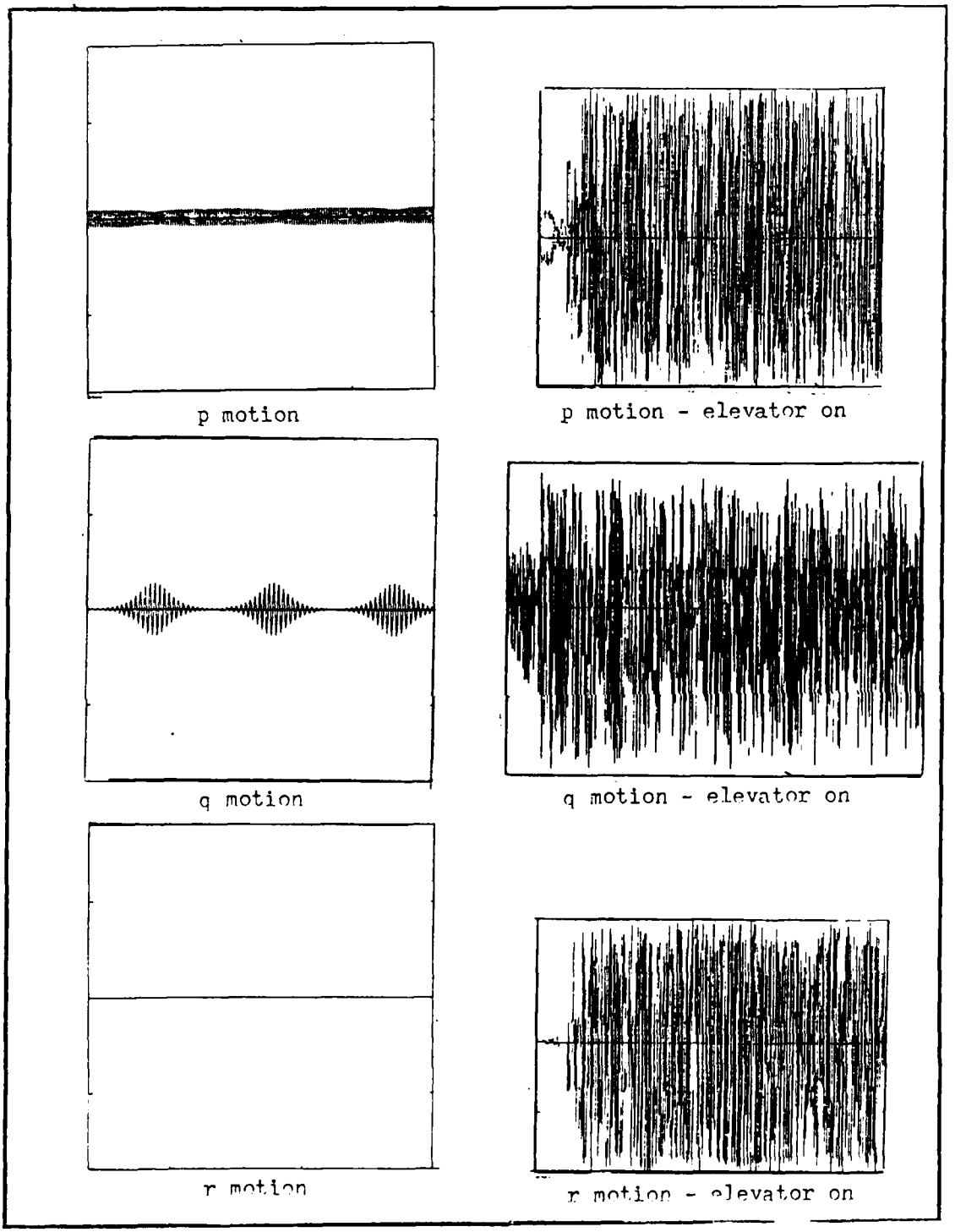

Fig. 22.

Effect of Elevator Motion on all 3 Axes

Appendix D

Appendix D contains the Fortran computer program used to numerically integrate Eqs (17a), (17b), (17c), (A-7a), (A-7b), (A-7c), and (A-7d).

```
      program space
      common /ham/ t,x(7,4),f(7,4),errest(7),n,h,i01,i02,i03,m,l1,
     +             w,e,sma,u,n4
      double precision t,x,f,errest,h,i01,i02,i03,m,l1,w,e,sma,u,n4,z,
     +                 phi,theta,psi,phidot,thetadot,psidot,phiplot,
     +                 thetaplot,psiplot,a,check,conversion,n4
      dimension z(7), a(3,3), phiplot(1750), thetaplot(1750),
     +  psiplot(1750)
c
c
c  variable descriptions
c
c  t is time
c  x is an array that is composed of 4 copies of the 7 state variables
c  f is the first time derivative of x
c  errest is needed for the haming differential equation integrator
c  n is number of equations as well as the number of variables
c  h is the integration timestep
c  i01, i02, & i03 are the static values of space station inertias
c  m is the mass of the elevator
c  l1 is the length of the space station along the yaw axis
c  w is the elevator frequency
c  e is the eccentricity of the orbit
c  sma is the semi-major axis of the orbit
c  u = GM is the earth's gravitational constant
c  n4 is the mean motion
c  z is just a storage place totally equivalent to x
c  phi, theta, & psi are the euler angles
c  phidot, thetadot, & psidot are the euler angle rates
c  phiplot, thetaplot, & psiplot are plotting storage places
c  a is the direction cosine matrix
c  check is a variable to validate quaternion accuracy
c
c
c
c  read in variables needed for master loops
      read (*,*) n, nprint, nstep
      read (*,*) t, h
c  nprint is the number of times data is printed (outer loop)
c  nstep is the number of steps or times haming is called
c  h is the integration step
c  total time of integration = nprint * nstep * h
c
c
c  read in static inertias, and m, l, w, e, sma, u, n4
      read (*,*) i01, i02, i03
      read (*,*) m, l1, w
      read (*,*) e, sma
      read (*,*) u
      n4 = sqrt(u/sma**3)
c
c  read in initial conditions
     read (*,*) phi, theta, psi
     read (*,*) phidot, thetadot, psidot
c
c  convert euler angles to radian measure
     conversion = 0.01745329
     phi = phi * conversion
```

```
      theta = theta * conversion
      psi = psi * conversion
      write (*,*) 'phi = ', phi, 'theta = ', theta, 'psi = ', psi
      write (*,*) '  '
c
c  compute initial direction cosine matrix (p5b)
      a(1,1) = cos(psi) * cos(phi) - sin(theta) * sin(psi) * sin(phi)
      a(1,2) = cos(psi) * sin(phi) + sin(theta) * sin(psi) * cos(phi)
      a(1,3) =-cos(theta) * sin(psi)
      a(2,1) =-cos(theta) * sin(phi)
      a(2,2) = cos(theta) * cos(phi)
      a(2,3) = sin(theta)
      a(3,1) = sin(psi) * cos(phi) + sin(theta) * cos(psi) * sin(phi)
      a(3,2) = sin(psi) * sin(phi) - sin(theta) * cos(psi) * cos(phi)
      a(3,3) = cos(theta) * cos(psi)
c
c  compute the initial angular velocity ( z(5), z(6), z(7) are w1,
c          w2, and w3, respectively )
      z(5) = a(1,3)*n4 + phidot*cos(theta)*sin(psi) + thetadot*cos(psi)
      z(6) = a(2,3)*n4 + phidot*sin(theta) + psidot
      z(7) = a(3,3)*n4 + phidot*cos(theta)*cos(psi) + thetadot*sin(psi)
c
c  compute initial quaternion (p5c)
      z(4) = 0.5 * sqrt( 1 + a(1,1) + a(2,2) + a(3,3) )
      z(1) = (0.25/z(4)) * ( a(2,3) - a(3,2) )
      z(2) = (0.25/z(4)) * ( a(3,1) - a(1,3) )
      z(3) = (0.25/z(4)) * ( a(1,2) - a(2,1) )
c
c  check sum of quaternion components squared being equal to one
      check = z(1)**2 + z(2)**2 + z(3)**2 + z(4)**2
c
c  print tabular headings and initial values
      write (*,*) '  '
      write (*,*) '  '
      write (*,11) t, (z(j), j=5,7), check, phi, theta, psi, phidot,
     +             thetadot, psidot
11    format (f9.1, 1x, 10(f9.6,1x))
c
c  rename variables for haming-suitable iteration
      x(1,1) = z(1)
      x(2,1) = z(2)
      x(3,1) = z(3)
      x(4,1) = z(4)
      x(5,1) = z(5)
      x(6,1) = z(6)
      x(7,1) = z(7)
c
c  initialize haming
      nxt = 0
      call haming(nxt)
      if(nxt .ne. 0) go to 50
1     format(2x,'haming did not initialize')
      write (*,1)
      stop
c
c
50    continue
c
c  integrate ordinary differential equations ... two nested loops
c
```

```
      do 200 ipr = 1, nprint
c
      do 100 istp = 1, nstep
c
           call haming(nxt)
c            each call to haming advances one step
c
100      continue
c         after nstep integration steps, convert to print variables and
c         print the current values
c
           z(1) = x(1,nxt)
           z(2) = x(2,nxt)
           z(3) = x(3,nxt)
           z(4) = x(4,nxt)
           z(5) = x(5,nxt)
           z(6) = x(6,nxt)
           z(7) = x(7,nxt)
c
c  compute dir cos matrix a, euler angles, & check quaternion (p5)
c  also, store data for plotter
      a(1,3) = 2 * ( z(1)*z(3) - z(2)*z(4) )
      a(2,1) = 2 * ( z(1)*z(2) - z(3)*z(4) )
      a(2,2) = -z(1)**2 + z(2)**2 - z(3)**2 + z(4)**2
      a(2,3) = 2 * ( z(2)*z(3) + z(1)*z(4) )
      a(3,3) = -z(1)**2 - z(2)**2 + z(3)**2 + z(4)**2
c
      phi = atan( -a(2,1)/a(2,2) )
      theta = asin( a(2,3) )
      psi = atan( -a(1,3)/a(3,3) )
c
      phiplot(ipr) = phi/conversion
      thetaplot(ipr) = theta/conversion
      psiplot(ipr) = psi/conversion
c
      phidot = ( (z(7)-a(3,3)*n4)*cos(psi) - (z(5)-a(1,3)*n4)*
     +          sin(psi) ) / cos(theta)
      thetadot=( (z(5)-a(1,3)*n4)*cos(psi) + (z(7)-a(3,3)*n4)*
     +          sin(psi) )
      psidot =   (z(6)-a(2,3)*n4) -
     +          ( (z(7)-a(3,3)*n4)*cos(psi) - (z(5)-a(1,3)*n4)*
     +          sin(psi) ) * tan(theta)
c
      check = z(1)**2 + z(2)**2 + z(3)**2 + z(4)**2
c
      write (*,11) t, (z(j), j=5,7), check, phi, theta, psi, phidot,
     +             thetadot, psidot
c
c
c
200   continue
c
c
c  output the euler angles so that an edited output file can be sent
c         to the plotter
c
      do 60 i = 1, nprint
      t = i * (h*nstep)
      write (*,85) t, phiplot(i)
60    continue
```

```
c
      do 70 i = 1, nprint
      t = i * (h*nstep)
      write (*,85) t, thetaplot(i)
70    continue
c
      do 80 i = 1, nprint
      t = i * (h*nstep)
      write (*,85) t, psiplot(i)
80    continue
c
85    format (f9.1, 3x, f20.13)
      stop
      end
c
c
c
c
c
      subroutine haming(nxt)
      common /ham/ x,y(7,4),f(7,4),errest(7),n,h,i01,i02,i03,m,l1,
     +             w,e,sma,u,n4
      double precision x,y,f,errest,h,xo,tol,hh,i01,i02,i03,m,l1,
     +                 w,e,sma,u,n4
      tol = 1.0d-08
      if(nxt) 190,10,200
10 xo = x
      hh = h/2.d+00
      call rhs(1)
      do 40 l = 2,4
      x = x + hh
      do 20 i = 1,n
20 y(i,l) = y(i,l-1) + hh*f(i,l-1)
      call rhs(l)
      x = x + hh
      do 30 i = 1,n
30 y(i,l) = y(i,l-1) + h*f(i,l)
40 call rhs(l)
      jsw = -10
50 isw = 1
      do 120 i = 1,n
      hh = y(i,1) + h*( 9.d+00*f(i,1) + 19.d+00*f(i,2) - 5.d+00*f(i,3)
     1     + f(i,4) ) / 24.d+00
      if( dabs( hh - y(i,2)) .lt. tol ) go to 70
      isw = 0
70 y(i,2) = hh
      hh = y(i,1) + h*( f(i,1) + 4.d+00*f(i,2) + f(i,3))/3.d+00
      if( dabs( hh-y(i,3)) .lt. tol ) go to 90
      isw = 0
90 y(i,3) = hh
      hh = y(i,1) + h*( 3.d+00*f(i,1) + 9.d+00*f(i,2) + 9.d+00*f(i,3)
     1     + 3.d+00*f(i,4) ) / 8.d+00
      if( dabs(hh-y(i,4)) .lt. tol ) go to 110
      isw = 0
110 y(i,4) = hh
120 continue
      x = xo
      do 130 l = 2,4
      x = x + h
130 call rhs(l)
```

```
      if(isw) 140,140,150
  140 jsw = jsw + 1
      if(jsw) 50,280,280
  150 x = xo
      isw = 1
      jsw = 1
      do 160 i = 1,n
  160 errest(i) = 0.0
      nxt = 1
      go to 280
  190 jsw = 2
      nxt = iabs(nxt)
  200 x = x + h
      npl = mod(nxt,4) + 1
      go to (210,230),isw
  210 go to (270,270,270,220),nxt
  220 isw = 2
  230 nm2 = mod(npl,4) + 1
      nml = mod(nm2,4) + 1
      npo = mod(nml,4) + 1
      do 240 i = 1,n
      f(i,nm2) = y(i,npl) + 4.d+00*h*( 2.d+00*f(i,npo) - f(i,nml)
     1     + 2.d+00*f(i,nm2) ) / 3.d+00
  240 y(i,npl) = f(i,nm2) - 0.925619835d+00*errest(i)
      call rhs(npl)
      do 250 i = 1,n
      y(i,npl) = ( 9.d+00*y(i,npo) - y(i,nm2) + 3.d+00*h*( f(i,npl)
     1     + 2.d+00*f(i,npo) - f(i,nml) ) ) / 8.d+00
      errest(i) = f(i,nm2) - y(i,npl)
  250 y(i,npl) = y(i,npl) + 0.0743801653d+00 * errest(i)
      go to (260,270),jsw
  260 call rhs(npl)
  270 nxt = npl
  280 return
      end
c
c
c
c
      subroutine rhs(nxt)
c
      common /ham/ t,x(7,4),f(7,4),errest(7),n,h,i01,i02,i03,m,ll,
     +             w,e,sma,u,n4
      double precision t,x,f,errest,h,i01,i02,i03,m,ll,w,e,sma,u,n4,
     +                 z,a,n4,rl,r,nl,n2,n3,i1,i2,i3,b
      dimension z(7), r(3), a(3,3)
c
c
c  variable description
c
c
c
c  calculate current values of inertia
      i1 = i01
      i2 = i02 + m * ( (0.5*ll*sin(w*t))**2 )
      i3 = i03 + m * ( (0.5*ll*sin(w*t))**2 )
c
c  once againe convert variable names
      z(1) = x(1,nxt)
      z(2) = x(2,nxt)
```

```
      z(3) = x(3,nxt)
      z(4) = x(4,nxt)
      z(5) = x(5,nxt)
      z(6) = x(6,nxt)
      z(7) = x(7,nxt)
c
c  calculate direction cosine matrix (p5)
      a(1,1) = z(1)**2 - z(2)**2 - z(3)**2 + z(4)**2
      a(1,2) = 2 * ( z(1)*z(2) + z(3)*z(4) )
      a(1,3) = 2 * ( z(1)*z(3) - z(2)*z(4) )
      a(2,1) = 2 * ( z(1)*z(2) - z(3)*z(4) )
      a(2,2) =-z(1)**2 + z(2)**2 - z(3)**2 + z(4)**2
      a(2,3) = 2 * ( z(2)*z(3) + z(1)*z(4) )
      a(3,1) = 2 * ( z(1)*z(3) + z(2)*z(4) )
      a(3,2) = 2 * ( z(2)*z(3) - z(1)*z(4) )
      a(3,3) = -z(1)**2 - z(2)**2 + z(3)**2 + z(4)**2
c
c  compute rl (length of orbit) (p15)
      rl = sma * (1 - e*cos(n4*t))
c
c  calculate radius vector components (p8)
      r(1) = a(1,1)*rl
      r(2) = a(2,1)*rl
      r(3) = a(3,1)*rl
c
c  calculate gravity gradient torque n (p7)
      b = (3*u) / (rl**5)
      n1 = b * (13-12) * r(2) * r(3)
      n2 = b * (11-13) * r(1) * r(3)
      n3 = b * (12-11) * r(1) * r(2)
c
c  write equations of motion (pp. 6a, 9b)
c
      f(1,nxt) = 0.5 * ( x(2,nxt)*(x(7,nxt)-a(3,3)*n4) - x(3,nxt)*
     +       (x(6,nxt)-a(2,3)*n4) + x(4,nxt)*(x(5,nxt)-a(1,3)*n4) )
c
      f(2,nxt) = 0.5 * (-x(1,nxt)*(x(7,nxt)-a(3,3)*n4) + x(3,nxt)*
     +       (x(5,nxt)-a(1,3)*n4) + x(4,nxt)*(x(6,nxt)-a(2,3)*n4) )
c
      f(3,nxt) = 0.5 * ( x(1,nxt)*(x(6,nxt)-a(2,3)*n4) - x(2,nxt)*
     +       (x(5,nxt)-a(1,3)*n4) + x(4,nxt)*(x(7,nxt)-a(3,3)*n4) )
c
      f(4,nxt) = 0.5 * (-x(1,nxt)*(x(5,nxt)-a(1,3)*n4) - x(2,nxt)*
     +       (x(6,nxt)-a(2,3)*n4) - x(3,nxt)*(x(7,nxt)-a(3,3)*n4) )
c
      f(5,nxt) = ( n1 + (i2-i3)*x(6,nxt)*x(7,nxt) ) / i1
c
      f(6,nxt) = ( n2 + (i3-i1)*x(7,nxt)*x(5,nxt) - (0.5*w*m*l1**2*
     +       sin(w*t)*cos(w*t)) * x(6,nxt) ) / i2
c
      f(7,nxt) = ( n3 + (i1-i2)*x(5,nxt)*x(6,nxt) - (0.5*w*m*l1**2*
     +       sin(w*t)*cos(w*t)) * x(7,nxt) ) / i3
c
      return
      end
```

Bibliography

1. Breakwell, J.V. and Ralph Pringle, Jr. "Nonlinear Resonance Affecting Gravity-Gradient Stability," International Astronautical Congress, Athens, Greece: 305-325 (September 1965).

2. Debra, Daniel B. and R.H. Delp. "Rigid Body Attitude Stability and Natural Frequencies in a Circular Orbit," Journal of the Astronautical Sciences, 8: 14-17 (Spring 1961).

3. Hayashi, Chihiro. Nonlinear Oscillations in Physical Systems. New York: McGraw-Hill Book Company, 1964.

4. Kane, Thomas R. and others. Spacecraft Dynamics. New York: McGraw-Hill Book Company, 1970.

5. Kaplan, Marshall H. Modern Spacecraft Dynamics & Control. New York: John Wiley & Sons, 1976.

6. Meirovitch, Leonard. Methods of Analytical Dynamics. New York: McGraw-Hill Book Company, 1970.

7. Salimov, G.R. "Motion of a Spacecraft Containing a Moving Element in a Gravitational Field," Mechanics of Solids, 9: 35-41 (1974).

8. Salimov, G.R. "Stability of Rotating Space Station Containing a Moving Element," Mechanics of Solids, 10: 52-56 (1975).

9. Wertz, James R. Spacecraft Attitude Determination and Control. Boston: D. Reidel Publishing Company, 1980.

VITA

Lieutenant John D. Chan was born on 3 October 1962 in Urbana, Illinois. He graduated from Central High School, Champaign, Illinois in 1980, and then attended the University of Illinois from which he received his Bachelor of Science degree in Aeronautical and Astronautical Engineering, May 1984. Upon graduation, he chose to enter Officer Training School and consequently received a commision in the USAF on 26 April, 1985. He then entered the School of Engineering, Air Force Institute of Technology, in June 1985.

Permanent Adress: 802 Haines Blvd.
Champaign, Illinois
61820

UNCLASSIFIED
SECURITY CLASSIFICATION OF THIS PAGE

REPORT DOCUMENTATION PAGE

Form Approved
OMB No. 0704-0188

1a. REPORT SECURITY CLASSIFICATION UNCLASSIFIED	1b. RESTRICTIVE MARKINGS
2a. SECURITY CLASSIFICATION AUTHORITY	3. DISTRIBUTION/AVAILABILITY OF REPORT Approved for public release; distribution unlimited
2b. DECLASSIFICATION/DOWNGRADING SCHEDULE	
4. PERFORMING ORGANIZATION REPORT NUMBER(S) AFIT/GA/AA/86D-2	5. MONITORING ORGANIZATION REPORT NUMBER(S)
6a. NAME OF PERFORMING ORGANIZATION School of Engineering 6b. OFFICE SYMBOL (If applicable) AFIT/ENG	7a. NAME OF MONITORING ORGANIZATION
6c. ADDRESS (City, State, and ZIP Code) Air Force Institute of Technology Wright-Patterson AFB, Ohio 45433	7b. ADDRESS (City, State, and ZIP Code)
8a. NAME OF FUNDING/SPONSORING ORGANIZATION 8b. OFFICE SYMBOL (If applicable)	9. PROCUREMENT INSTRUMENT IDENTIFICATION NUMBER
8c. ADDRESS (City, State, and ZIP Code)	10. SOURCE OF FUNDING NUMBERS PROGRAM ELEMENT NO. / PROJECT NO. / TASK NO / WORK UNIT ACCESSION NO

11. TITLE (Include Security Classification)
AN ANALYSIS OF SPACE STATION MOTION SUBJECT TO THE PARAMETRIC EXCITATION OF PERIODIC ELEVATOR MOTION

12. PERSONAL AUTHOR(S)
John D. Chan, 2d Lt, USAF

13a. TYPE OF REPORT	13b. TIME COVERED	14. DATE OF REPORT (Year, Month, Day)	15. PAGE COUNT
MS Thesis	FROM _____ TO _____	1986 December	82

16. SUPPLEMENTARY NOTATION

17. COSATI CODES			18. SUBJECT TERMS (Continue on reverse if necessary and identify by block number)
FIELD	GROUP	SUB-GROUP	
22	01		Astronautics, Satellite Attitude
22	02		Space Stations

19. ABSTRACT (Continue on reverse if necessary and identify by block number)

Thesis Advisor: Curtis H. Spenny
Assistant Professor of Aerospace and Systems Engineering

Abstract on Back

Approved for public release: IAW AFR 190-1
13 May 87
Dean for Research and Development
Air Force Institute of Technology (AU)
Wright-Patterson AFB OH 45433

20. DISTRIBUTION/AVAILABILITY OF ABSTRACT ☒ UNCLASSIFIED/UNLIMITED ☐ SAME AS RPT ☐ DTIC USERS	21. ABSTRACT SECURITY CLASSIFICATION UNCLASSIFIED
22a. NAME OF RESPONSIBLE INDIVIDUAL Curtis H. Spenny, Professor	22b. TELEPHONE (Include Area Code) 513-255-3517 / 22c. OFFICE SYMBOL AFIT/ENG

DD Form 1473, JUN 86 Previous editions are obsolete

SECURITY CLASSIFICATION OF THIS PAGE
UNCLASSIFIED

The future space station will contain an elevator mechanism that will transport mass between the separate compartments. Accordingly, this study will derive the equations of attitude motion for a gravity gradient stabilized space station whose moments of inertia are varying with time. The equations are then linearized, after which an analytical solution of the pitch equation is developed. An examination of the stability of motion for the resulting Hill equation is presented and then compared to the solution obtained from numerical integration of the nonlinear equations. The results show that for elevator frequencies on the order of the orbit rate, motion can grow unboundedly with time. Consequently, the shape of the classical Lagrange stability region is altered.

END

5-87

DTIC